Left-right asymmetry in heart development and disease: forming the right loop

Audrey Desgrange, Jean-François Le Garrec, Sigolène Meilhac

© 2018. Published by The Company of Biologists Ltd | Development (2018) 145, dev162776. doi:10.1242/dev.162776

REVIEW

Left-right asymmetry in heart development and disease: forming the right loop

Audrey Desgrange[1,2], Jean-François Le Garrec[1,2] and Sigolène M. Meilhac[1,2,*]

ABSTRACT

Extensive studies have shown how bilateral symmetry of the vertebrate embryo is broken during early development, resulting in a molecular left-right bias in the mesoderm. However, how this early asymmetry drives the asymmetric morphogenesis of visceral organs remains poorly understood. The heart provides a striking model of left-right asymmetric morphogenesis, undergoing rightward looping to shape an initially linear heart tube and align cardiac chambers. Importantly, abnormal left-right patterning is associated with severe congenital heart defects, as exemplified in heterotaxy syndrome. Here, we compare the mechanisms underlying the rightward looping of the heart tube in fish, chick and mouse embryos. We propose that heart looping is not only a question of direction, but also one of fine-tuning shape. This is discussed in the context of evolutionary and clinical perspectives.

KEY WORDS: Heart looping, Heart morphogenesis, Heterotaxy, Left-right asymmetry

Introduction

The heart is an asymmetric organ. In humans, it is positioned on the left side of the thoracic cavity. In addition, it is partitioned in two halves, driving a double blood circulation. The atrial and ventricular chambers, as well as the great vessels, in the left and right halves of the heart have distinct anatomical features, which are adapted to the systemic and pulmonary circulation, respectively (Jacobs et al., 2007; Van Praagh, 2006). Thus, the position and alignment of the cardiac segments are crucial for heart function. This is prefigured in the embryo, during the process of heart looping. The rightward looping of the heart primordium is the first sign of asymmetric organogenesis. It corresponds to the transformation of a straight cardiac tube into a loop (Fig. 1), which is either a flat-S in the fish or a helix in amniotes (chick and mouse). By determining the relative position of cardiac chambers, heart looping in amniotes is essential for the asymmetric partition of the heart. Failure to complete the partition of the heart leads to incorrect oxygenation of the blood. Accordingly, abnormal left-right patterning of the heart is associated with severe congenital heart defects, as exemplified in heterotaxy syndrome.

Work in experimental models has been essential for understanding the mechanisms underlying left-right asymmetric morphogenesis. Breaking of the bilateral symmetry of the vertebrate embryo was shown to take place in the left-right organiser (see Glossary, Box 1), resulting in asymmetric signalling of the left determinant Nodal, a secreted factor of the TGFβ family (see Nakamura and Hamada, 2012) (Fig. 2, step 1). However, the initial bias in a tissue (organiser) that does not contribute to visceral organs (Sulik et al., 1994) does not explain the asymmetric morphogenesis of specific organs. Thus, how the initial molecular asymmetry is sensed by organ precursor cells and modulates morphogenesis has remained poorly understood. Brown and Wolpert (1990) hypothesised that a second step is required (Fig. 2, step 2), in which the initial molecular asymmetry biases a morphogenetic process to generate an asymmetric shape. This process is referred to as an organ-specific random generator of asymmetry: specific because the mechanism may differ between organs; random because, in the absence of the bias, it can generate random asymmetric shapes. Since its first description by embryologists of the 19th century, heart looping has been mainly considered in the literature as a directional problem (rightward, leftward, undetermined) and a simple readout of the symmetry-breaking event. However, recent studies using genetic manipulations, cell tracing and 3D quantifications have provided novel insights into the morphogenetic process of heart looping and the fine geometry of the looped heart tube. This raises the possibility of characterising the heart-specific random generator of asymmetry.

Here, we summarise current knowledge on the mechanisms of asymmetric heart morphogenesis, with a focus on heart looping. We begin by considering general principles of morphogenesis, explaining how intrinsic and extrinsic mechanisms can generate the looping of a tube, and how computer simulations can provide further insight into these mechanisms. We then review the spatio-temporal dynamics of left-right asymmetries during heart development. By comparing three different animal models – fish, chick and mouse – we discuss the cellular and molecular mechanisms that may contribute to a heart-specific generator of asymmetry and we consider its evolutionary conservation. Finally, we present the cardiac malformations that are currently associated with laterality defects in humans.

Intrinsic and extrinsic mechanisms of tube looping

The emergence of biological form involves the integration of local regulation of tissue growth with mechanical constraints from the neighbouring regions to which the tissue is connected. These two aspects are referred to as intrinsic and extrinsic mechanisms of morphogenesis. In the context of the deformation of a tubular organ, intrinsic mechanisms correspond to the behaviour of cells within the tube, whereas extrinsic mechanisms refer to external forces acting on the tube, e.g. those at the borders of the tube or those resulting from embryonic processes outside the tube.

In the case of intrinsic mechanisms, tissue growth can be regulated both in terms of its rate and its orientation (Kennaway et al., 2011). Growth rate is considered at the tissue scale, and may result from either cell proliferation or an increase in cell size. Growth orientation implies that cells are able to perceive a reference axis, at the tissue or embryonic level, such that the tissue is polarised and cells orient their

[1]*Imagine*-Institut Pasteur, Laboratory of Heart Morphogenesis, 75015 Paris, France. [2]INSERM UMR1163, Université Paris Descartes, 75015 Paris, France.

*Author for correspondence (sigolene.meilhac@institutimagine.org)

S.M.M., 0000-0003-4080-2617

Development (2018) 145, dev162776. doi:10.1242/dev.162776

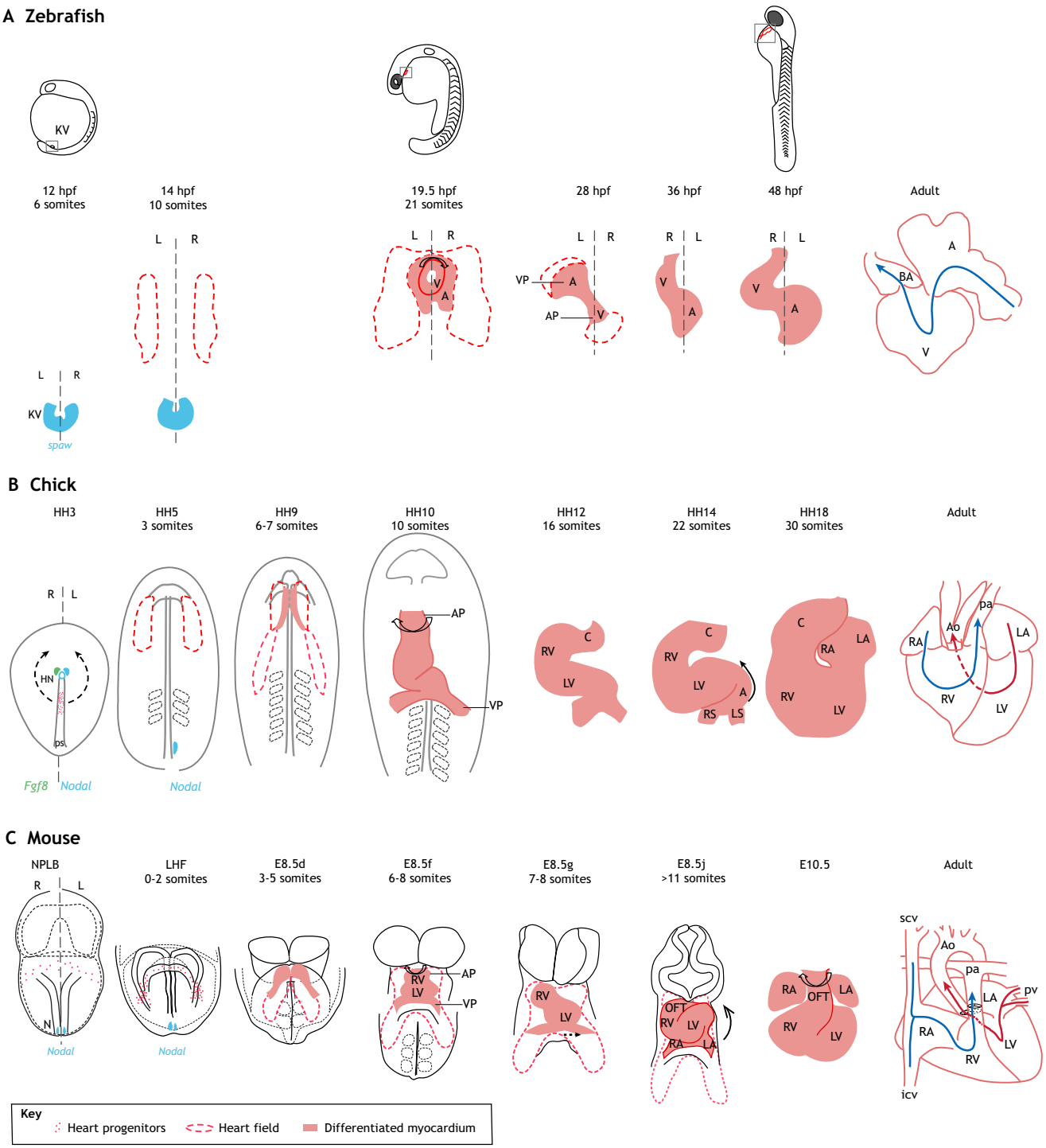

Fig. 1. Stages of asymmetric heart morphogenesis in different vertebrate models. Overview of heart morphogenesis, showing molecular left-right asymmetries, the position of the field of heart precursor cells and morphological changes from the formation of the heart tube to the mature heart. Blood circulation in the mature heart is shown by coloured lines (blue, carbonated blood; red, oxygenated blood). Similar stages are compared between the zebrafish (A), chick (B) and mouse (C). In A, lateral views of zebrafish embryos in the upper panels illustrate that imaging is easier dorsally at early stages and ventrally at later stages. Thus, dorsal (14-28 hpf) and ventral (36-48 hpf) views of the heart region are shown in the lower panels. In B and C, ventral views are shown. A, atrium; Ao, aorta; AP, arterial pole; BA, bulbus arteriosus; C, conus; HN, Hensen's node; icv, inferior caval vein; KV, Kupffer's vesicle; L, left; LA, left atrium; LHF, late headfold stage; LS, left sinus venosus; LV, left ventricle; N, node; NPLB, neural plate late bud stage; OFT, outflow tract; pa, pulmonary artery; ps, primitive streak; pv, pulmonary veins; R, right; RA, right atrium; RS, right sinus venosus; RV, right ventricle; scv, superior caval vein; V, ventricle; VP, venous pole.

behaviour accordingly. Such behaviours can be computationally simulated to assess how tube deformations might be generated; potential models of tube deformation can thereby be postulated (Fig. 3). In a differential growth model (Fig. 3A), the rate of tissue growth varies both along the length and around the circumference of the tube. It is possible to define a pattern of growth zones (with a

Development (2018) 145, dev162776. doi:10.1242/dev.162776

Box 1. Glossary

Buckling: A mechanical instability, characterised by a sudden sideways deformation. It applies to the growth of the heart tube, when constrained between fixed poles, and thus undergoes looping as a result of buckling (also see Fig. 3).

Chirality: From the Greek 'hand', describes the asymmetric property of objects, such as the hand, which cannot be superimposed on their mirror image.

Convergence-extension: The process by which cells within a tissue converge along one axis and extend along a perpendicular axis. This process drives tissue deformation during organogenesis, with a combined narrowing on one axis and elongation perpendicularly.

Dorsal mesocardium: A dorsal tissue in amniotes, which initially attaches the heart tube to the dorsal pericardial wall, beneath the foregut. It is progressively broken during heart looping, corresponding to dorsal closure of the heart tube.

Heart field: The embryological concept of a field refers to a population of cells at a particular location that will give rise to a tissue or organ during development; thus, a heart field is a source of cardiac precursor cells. Two heart fields have been characterised, the first and second heart fields, with sequential timing of ingression through the primitive streak at gastrulation, distinct spatial distribution at the time of the formation of the heart tube and sequential timing of differentiation corresponding to sequential integration into the heart tube.

Isomerism: From the Greek 'equal parts', refers to the development of anatomical structures, which normally have a specific arrangement on the left or right side, in pathological conditions in which they adopt a bilateral symmetry. Left and right isomerism corresponds to bilateral left and right structures, respectively.

Lateral plate mesoderm (LPM): Subdivision of the mesoderm after gastrulation, based on its position further away from the midline. It contains precursor cells of the heart, vessels and blood, as well as of the limb skeleton, craniofacial skeletal muscles, the mesenteries, and the lining of the pleural, cardiac and abdominal cavities.

Left-right organiser: Transient anatomical structure in which the left-right symmetry of the embryo is initially broken. Based on structural differences, it has specific names in different species – the node in mammals, Hensen's node in the chick and Kupffer's vesicle in the fish (see also Fig. 1).

Situs: From the Latin 'position', this term is used to describe whether the arrangement of visceral organs or heart segments is normal (situs solitus), mirror-imaged (situs inversus) or incoherent (situs ambiguus or heterotaxy).

higher growth rate, but a constant orientation, along the axis of the tube) able to generate tube looping. In an oriented growth model (Fig. 3B), the rate of growth is the same around the circumference of the tube, but the orientation of growth, which is tilted relative to the tube axis, can generate looping. Although these models provide insight into how intrinsic mechanisms might contribute to tube looping, their existence should be demonstrated experimentally, based on the correct morphogenesis of the isolated tube. In addition, local molecular regulations of tissue growth are expected to intervene. Such intrinsic mechanisms have been demonstrated in the case of the fly hindgut, which undergoes a counterclockwise rotation. Here, epithelial cells are chiral, showing both apico-basal polarity and left-right asymmetric shape; computer simulations have shown that the introduction and subsequent dissolution of this chirality (see Glossary, Box 1), followed by a process of chiral cell sliding (i.e directional change of a cell position relative to its neighbours), are sufficient to induce tube rotation (Inaki et al., 2018; Taniguchi et al., 2011). Cell chirality in this context is associated with the polarisation of E-cadherin at cell boundaries and is regulated by components of the planar cell polarity (PCP) pathways, whereas the initial left-right bias is provided by the atypical myosin MyoID within a hindgut-specific organiser (González-Morales et al., 2015).

Extrinsic mechanisms can also drive tube looping and have, for example, been shown to participate in the direction of gut rotation in the chick. The dorsal mesentery of the chick gut displays left-right asymmetry in its cellular architecture, which is dependent on the left determinants Nodal/Pitx2. This drives tilting of the dorsal mesentery, thus exerting forces on the gut tube attached to it (Davis et al., 2008). Convergence-extension (see Glossary, Box 1) is another mechanism that can contribute to the growth of tubular structures, such as the trachea and hindgut in flies, or the kidney and cochlea in vertebrates (Chen et al., 1998; Iwaki and Lengyel, 2002; Karner et al., 2009; Wang et al., 2005). This process describes the behaviour of precursor cells outside the tube, while they integrate in the tube and, as such, can be considered as an extrinsic mechanism of tube morphogenesis. Another simple extrinsic mechanism, termed buckling (see Glossary, Box 1), was proposed to function in the context of the heart, based on morphological observations more than a century ago (His, 1868; Patten, 1922). This mechanism can also be illustrated by computer simulations showing that, when the cardiac tube grows longitudinally, with a fixed distance between its poles, it will deform. The precise shape derived from such a buckling process may be biased by small asymmetries at the tube poles, in terms of growth rates (Fig. 3C) or rotation of the tube (Le Garrec et al., 2017). Experimentally, the existence of extrinsic mechanisms can be inferred from the culture of isolated tubes, which do not develop correctly. In addition, regulation of asymmetries is expected to occur outside the tube.

In both cases of intrinsic and extrinsic mechanisms, computer simulations have shown that the geometry of growth patterns is important to determine whether the final tube adopts a helical shape or a flat-S shape. If the growth patterns are within the same plane together with the tube axis, the tube will deform in 2D, and generate a flat-S shape, as in the case of the fish heart (Fig. 3Aii,Bii,Cii). By contrast, a helical shape, as observed in the amniote heart, requires breaking this planar configuration. This may occur through different means: by introducing a third zone of differential growth (Fig. 3Ai), a 120° separation, over the circumference, between the zones defining the orientation bias (Fig. 3Bi) or between the asymmetries influencing buckling (Fig. 3Ci).

Overall, these types of computer simulations highlight potential mechanisms that might underlie a heart-specific random generator of asymmetry, in the sense of Brown and Wolpert (1990). In the next sections, we use this framework to summarise current knowledge on the mechanism of heart looping in three animal models: zebrafish, chick and mouse. As formation of the muscular tube is associated with the differentiation of progenitor cells, outside the tube, into myocardial cells, inside the tube, we define as intrinsic the mechanisms driven by the behaviour of cardiomyocytes. However, this classification, which is useful conceptually, does not take into consideration the continuum of biological processes that occur during tube looping, such as cell differentiation at the points of attachment of the tube. In addition, intrinsic and extrinsic mechanisms are not mutually exclusive and may well occur synergistically to drive morphogenesis.

Left-right asymmetric heart morphogenesis in the zebrafish

In the zebrafish, the heart tube forms between 22 and 24 h post fertilisation (hpf) via the fusion of bilateral cardiac cell populations of the lateral plate mesoderm (LPM; see Glossary, Box 1), assembled into a disc. From the disc, a cone-shaped intermediate forms and then telescopes out into a tube (Stainier et al., 1993) (Fig. 4). As the tube undergoes elongation, its venous end is displaced towards the left in an asymmetric process referred to as

Development (2018) 145, dev162776. doi:10.1242/dev.162776

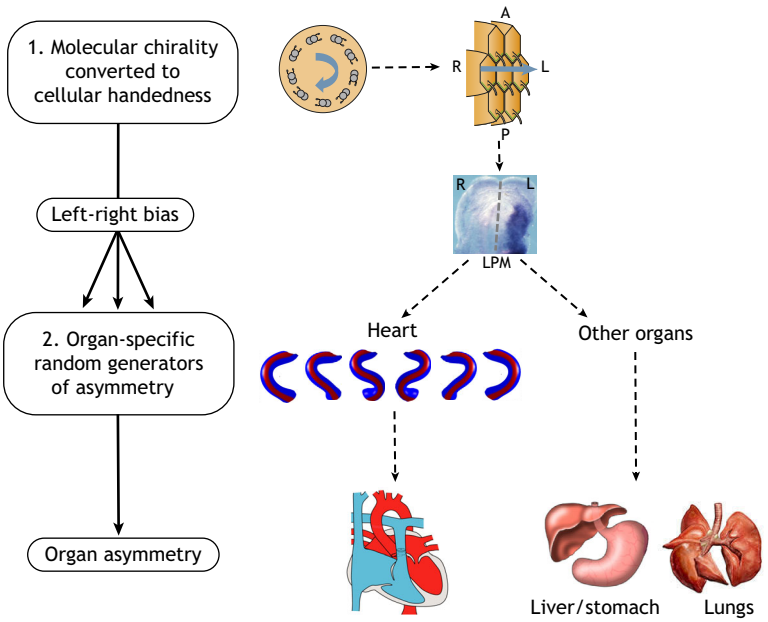

Fig. 2. The Brown and Wolpert model of a two-step mechanism underlying the left-right asymmetry of visceral organs. (1) In the first step, molecular chirality is converted into handedness at the cellular level (Brown and Wolpert, 1990). This theory was confirmed by later experimental work, providing a biological mechanism. In the mouse left-right organiser, chirality of the tubulin polymers in ciliary microtubules (left panel), as well as planar alignment of the basal bodies in node cells, determine the direction of a fluid flow (right panel) (see Satir, 2016). A, anterior; L, left; P, posterior; R, right. This results in asymmetric gene expression in the lateral plate mesoderm (LPM) (Nonaka et al., 1998), thus providing a genetic bias between left and right cells. (2) In the second step, the left-right bias influences an organ-specific random generator of asymmetry. In the context of the heart, it has been proposed that a buckling mechanism is able to generate random deformations of the heart tube (Le Garrec et al., 2017). However, during normal development, this mechanism is biased at the poles to consistently generate a rightward looping. The left-right bias is established once and can be used to orient several organ-specific generators of asymmetry along the same reference, thus leading to a single configuration of organ situs. Images of the liver, stomach and lungs are reproduced from Anderson et al., 2018 with permission.

cardiac jogging (Chen et al., 1997). The left shift of the venous pole is visible until 28 hpf, as the heart tube is later progressively repositioned towards the midline (Chin et al., 2000). From 30 hpf, the ventricular chamber starts to bend rightwards, a process referred to as cardiac looping. In combination with the formation of a constriction at the atrio-ventricular region and the expansion of the outer curvature of the cardiac chambers, the axis of the looped heart in zebrafish takes the shape of a flat-S at 48 hpf.

In recent years, lineage-tracing and live-imaging approaches have provided valuable insights into the cellular behaviour that drive the stages of asymmetric heart morphogenesis. Although the lineage tracing of left versus right heart precursors at gastrulation stages did not reveal any difference in their relative cell contributions, in terms of numbers or ventricular/atrial fate (Keegan et al., 2004), mapping the expression domain of the left marker *lefty2* (*lft2*) or the lineage tracing of left cells at the disc stage, revealed a specific contribution of these cells to the dorsal heart tube at the jogging stage at 24 hpf (Baker et al., 2008; Rohr et al., 2008; Smith et al., 2008). This is in keeping with the observations that right cells involute during jogging, such that they are displaced ventrally, with a temporal sequence starting with ventricular cells followed by atrial cells. In mutants with left-right patterning defects, the initial point of involution is incorrectly specified (Rohr et al., 2008), highlighting how cardiac jogging is controlled by left-right patterning. Live imaging has revealed that the migration of myocardial cells in the disc/cone also contributes to asymmetric morphogenesis. Initially, differential speed migration is observed with an anterior/posterior, rather than left/right, regionalisation (de Campos-Baptista et al., 2008; Smith et al., 2008). Cells then migrate towards the anterior and the left, with higher speed and displacement observed for posterior cells, thus underlying a 30° clockwise rotation of the cardiac cone viewed dorsally (Baker et al., 2008; de Campos-Baptista et al., 2008; Rohr et al., 2008; Smith et al., 2008). More recently, mathematical modelling has indicated that such differential cell motility is sufficient to account for cardiac jogging (Veerkamp et al., 2013). Given that these types of behaviour concern cells that are already differentiated, i.e. expressing *myl7* (also known as *cmlc2*), they can be considered as intrinsic mechanisms that drive the asymmetric morphogenesis of the cardiac tube during the jogging phase.

Longer-term tracing of left cells in the disc has highlighted a left contribution to the looped heart at 48 hpf, following the dorsal contribution at 24 hpf, which indicates a second phase of tissue rotation between the jogging and looping stages (Baker et al., 2008). Based on the spiralling of lefty 2 labelling at the tube poles, others have suggested a torsion, rather than a rotation, between the jogging and the looped stages (Smith et al., 2008). However, the mechanism underlying this further deformation has not been characterised. Explant experiments have shown that heart looping can proceed in isolation, again supporting intrinsic mechanisms. Based on pharmacological treatments of explanted hearts, zebrafish looping was suggested to depend on the actomyosin cytoskeleton (Noël et al., 2013). Furthermore, differential cell shapes have been observed in the outer and inner curvatures of cardiac chambers and are proposed to contribute to chamber shape (Auman et al., 2007; Rohr et al., 2008); cells in the latter are cuboidal, whereas cells of the former, which express Nppa, flatten and elongate between 27 hpf and 52 hpf, thereby causing expansion of the outer curvature. Cell elongation in the ventricle tends to be perpendicular to the arterial-venous axis of the cardiac tube. These cell shape changes in the outer curvature depend on the redistribution of F-actin (Deacon et al., 2010), which was recently shown to be under the control of PCP signalling (Merks et al., 2018). Thus, expansion of cardiac chambers – with the ventricle curving on the right and the atrium on the left – may contribute to the looped shape of the zebrafish heart.

Extrinsic mechanisms may also influence asymmetric heart morphogenesis in zebrafish, although they remain poorly characterised. Between 20 hpf and 48 hpf, the heart tube grows about 3.6-fold, from 85 to 310 cells (de Pater et al., 2009; Grant et al., 2017), reaching a tube length of 150 µm by 24 hpf (Veerkamp et al., 2013). However, cell proliferation is low within the tube itself and high at the poles of the heart or in the precursor cells of the LPM (de Pater et al., 2009). These observations indicate that heart tube elongation during jogging involves cell recruitment. In line with this, it has been shown that the heart field (see Glossary, Box 1), which can be traced by the expression of Hand2, Isl1, Nkx2-5 or Tbx1, before and after heart tube formation (de Pater et al., 2009; Felker et al., 2018; Fukui et al., 2018; Hami et al., 2011; Lazic and Scott, 2011; Paffett-Lugassy et al., 2013; Schoenebeck et al., 2007; Zhou et al., 2011), is less visible by the time of heart looping

Development (2018) 145, dev162776. doi:10.1242/dev.162776

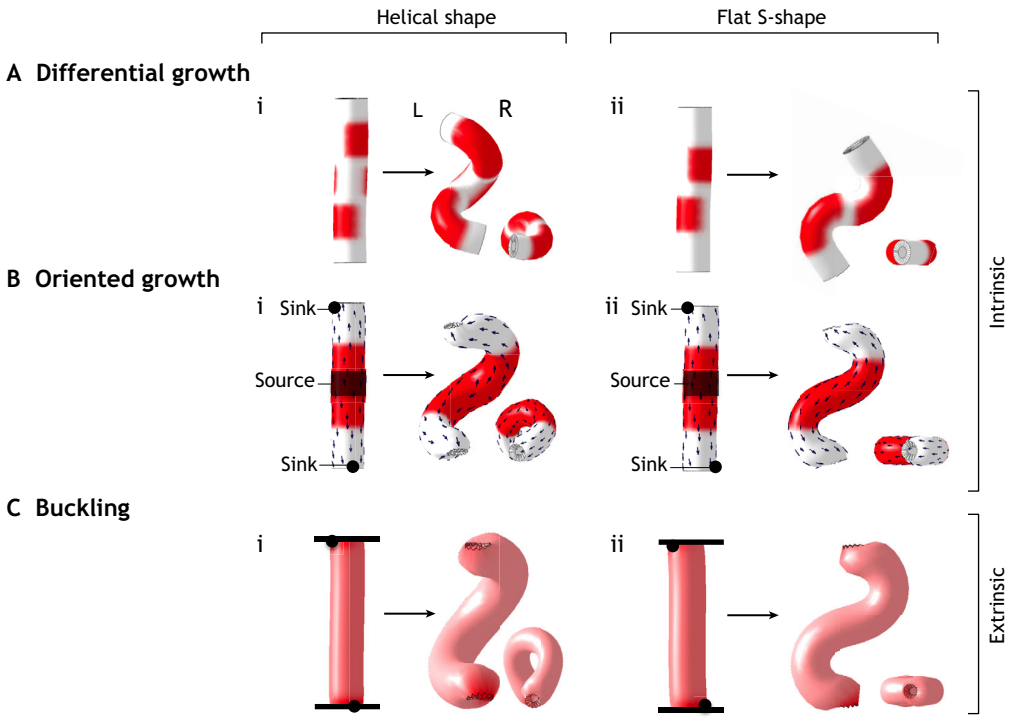

Fig. 3. Theoretical intrinsic and extrinsic mechanisms of tube looping. Simulations of tube looping with a finite element model (described by Le Garrec et al., 2017). Three looping mechanisms (differential growth, oriented growth or buckling; A-C) were implemented, with either a setting in three dimensions (Ai,Bi,Ci) or 2 dimensions (Aii,Bii,Cii), generating a helical shape, as seen in the amniote heart, or a flat-S shape, as seen in the fish heart, respectively. For each mechanism, the initial condition is shown (left) alongside the output shape, seen from a dorsal view (middle) and a cranial view (right). (A) Differential growth within the heart tube. A helical shape (Ai) can be generated from higher (dark red) longitudinal growth (i.e. along the tube axis) in three bands, positioned along the length of the tube, in a helical configuration (right in the upper band, ventral in the middle band, left in the lower band). A flat-S shape (Aii) can be generated from two bands of higher longitudinal growth, positioned on each side (left/right) of the tube. (B) Oriented growth within the heart tube. The simulations assume a uniform growth rate in a large band (red). The direction of growth is oriented (black arrows) from a morphogen, synthesised at a central source and degraded in two sinks, at each pole of the tube. In the 3D setting (Bi), the sinks are positioned at 120° relative to each other, leading to a helical shape. In the 2D setting (Bii), the sinks are positioned on each side of the tube, leading to a flat-S shape. (C) Buckling, as an example of an extrinsic mechanism. Contrary to the previous simulations, the two poles of the tube are fixed in all three directions (black bars). The rate of growth is uniform along the tube, except in a small region at each pole, with higher growth. In the 3D setting (Ci), regions with higher growth are positioned at 120° relative to each other, producing a helix. In the 2D setting (Cii), regions of higher growth are positioned on each side (left/right) of the tube, generating a flat S.

(Fig. 4). However, whether cell recruitment is asymmetric is an unresolved issue. The asymmetric expression of the actin gene *acta1b* in the left side of the cone at 21 hpf (Noël et al., 2013), or the higher number of cells expressing *prrx1a* and *tbx5* in the right LPM (Ocaña et al., 2017) may potentially reflect differences in cell proliferation and differentiation. In addition, a line of *tbx5*-positive cells, expressing markers of actomyosin and thus referred to as a cable, has been detected on the right side of the heart tube at 30 hpf (Ocaña et al., 2017). However, whether this structure underlies tension and asymmetric morphogenesis in this context remains to be demonstrated.

Asymmetric heart morphogenesis is preceded by asymmetric gene expression. The first gene to be asymmetrically expressed in the left LPM is the Nodal-related gene *spaw*, which is expressed caudally at the 10-somite stage and then propagates cranially; by contrast, the *oep* gene, which encodes the Nodal co-receptor, is bilaterally expressed in the same region (Long et al., 2003; Noël et al., 2013). At the disc stage (21 somites), targets of Nodal signalling are activated on the left side. These include the Nodal-related gene *cyc*, and *lefty2*, which encodes a Nodal antagonist, both of which are expressed in a region overlapping with cardiomyocytes of the cardiac disc, but adjacent to that of *spaw* expression (Fig. 4). Another Nodal target gene, encoding the transcription factor Pitx2c, is activated in the left LPM (Noël et al., 2013) when *spaw* is turned off at the 25-somite stage. *lefty2* is then expressed in the dorsal part of the heart tube at 24 hpf. Bmp signalling is known to follow on from Nodal signalling, although whether it is also asymmetric is controversial. *bmp4* was found to be more highly expressed in the left side of the disc at the 22-somite stage, and remains expressed in the left side of the heart tube at 24 hpf (Bisgrove et al., 2000; Chen et al., 1997; Chocron et al., 2007). In addition, the BMP effectors phospho-smad 1/5/8 are enriched on the left side of the cone at the 23-somite stage (Smith et al., 2008), mainly in endocardial cells (Lenhart et al., 2013). However, in another study, *bmp4* expression was found to be symmetric in the disc at 19 hpf, with phospho-smad 1/5/8, and a Bmp reporter transgene, enriched on the right side (Veerkamp et al., 2013). These analyses of gene or signalling profiles are currently based on 2D images. Given the important changes in geometry during the growth of the cone and elongation of the tube, 3D analyses would help to resolve the observed discrepancies. Other asymmetric markers include phosphorylated non muscle myosin 2 (*myh9a*), which is enriched in the right side of the cone at 20.5 hpf (Veerkamp et al., 2013), and *has2*, which encodes an enzyme involved in remodelling the extracellular matrix (ECM). *has2*, which is expressed in the left side of the cone at the 25-somite stage, was shown to be an effector of Nodal and Bmp

Development (2018) 145, dev162776. doi:10.1242/dev.162776

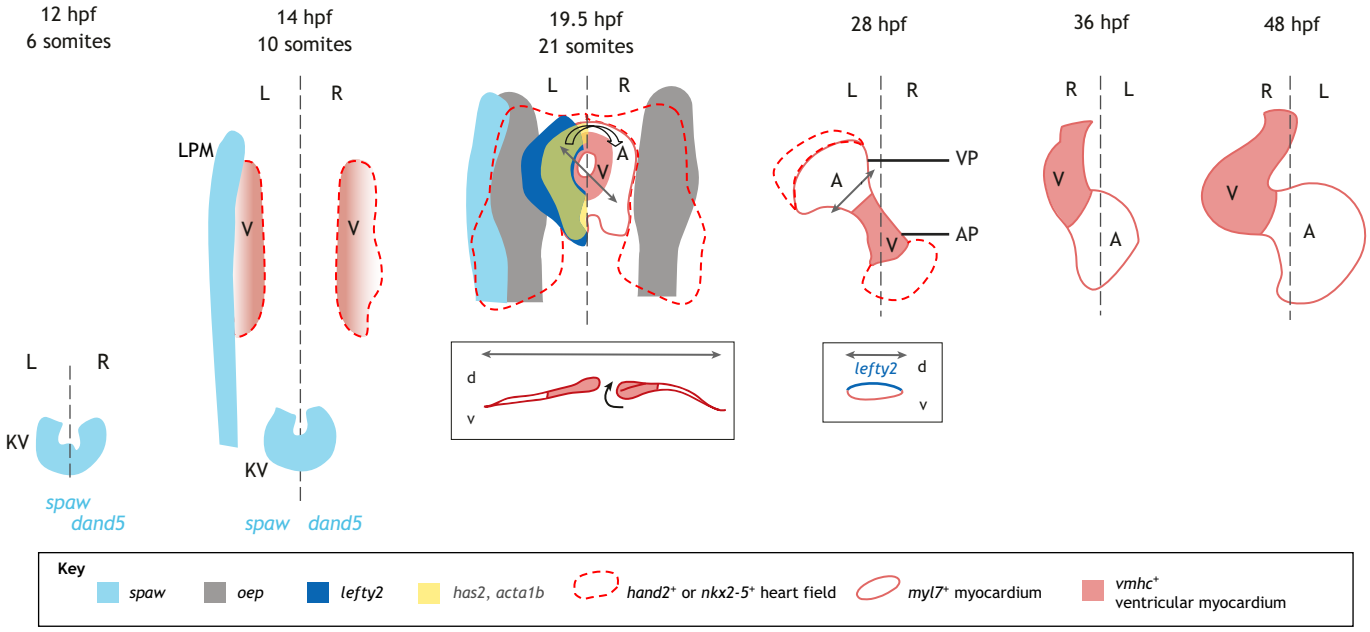

Fig. 4. Left-right asymmetric patterning and looping of the heart in the zebrafish. In the zebrafish, asymmetric gene expression (e.g. *dand5*) is first seen (at 12 hpf) in the left-right organiser (the Kupffer's vesicle) and then (e.g. *spaw* at 14 hpf) in the lateral plate mesoderm (LPM). In the bilateral heart field at 14 hpf (red dotted line), cardiomyocytes expressing *myl7* differentiate (red), with ventricular cells (V), expressing *vmhc*, lying medially to atrial cells (A). The formation and rotation (thick arrow) of the cardiac disc (19.5 hpf) is followed by the extension of the cardiac tube (28 hpf), with a leftward displacement of the venous pole. Heart looping is a later event, when the tube bends in a C-shape (36 hpf) and finally acquires an S-shape (48 hpf). The patterns of gene expression are colour coded. Double-headed arrows indicate the location of the sections shown underneath. At 19.5 hpf, the curved arrow indicates the direction of cell involution. Dorsal (14-28 hpf) and ventral (36 and 48 hpf) views are shown, following how the heart is imaged. Anterior and posterior are represented at the top and bottom, respectively. A, atrium; AP, arterial pole; d, dorsal; KV, Kupffer's vesicle; L, left: R, right; v, ventral; V, ventricle; VP, venous pole.

signalling in heart jogging (Smith et al., 2008; Veerkamp et al., 2013).

Mutant analyses have demonstrated a requirement for Nodal, Bmp and Shh signalling during asymmetric heart morphogenesis. Embryos morphant or mutant for *spaw* have disrupted cardiac jogging, with no obvious direction, in 30-60% of cases, and this is accompanied by randomised positioning of the pancreas, gut and epithalamus nuclei (Long et al., 2003; Noël et al., 2013; Lenhart et al., 2013). In these mutant embryos, the expression of *spaw*, consistent with its auto-activation and that of its targets *cyc*, *lefty2* and *pitx2c*, are lost in the LPM. Mutations for other components of the Nodal pathway, such as the co-receptor Oep or the transcriptional effector Foxh1, lead to a similar phenotype (Bisgrove et al., 2000; de Campos-Baptista et al., 2008; Lenhart et al., 2013; Yan et al., 1999), whereas *pitx2* is not required for either jogging or looping (Ji et al., 2016). Cardiomyocytes in late zygotic *oep* or *spaw* mutants move with a reduced and homogenous speed and reduced directionality during the formation of the cardiac cone, thus preventing its rotation (de Campos-Baptista et al., 2008; Noël et al., 2013). In *spaw* morphants, in a *bmp4* mutant background, disruption of cardiac jogging is exacerbated, such that 90% of cases have no obvious direction of jogging (Lenhart et al., 2013). Bmp signalling downstream of Nodal (Lenhart et al., 2013; Veerkamp et al., 2013) is similarly required for the differential speed and directionality of cardiomyocyte migration that underlies the rightward rotation of the disc (Smith et al., 2008). Local changes in Bmp signalling, induced by beads implanted in the LPM or by Spaw-expressing cardiomyocyte clones, can dictate the direction of cardiac jogging (Smith et al., 2008; Veerkamp et al., 2013). It has also been shown that Bmp and Shh signalling are required for heart looping, acting to control cardiomyocyte differentiation and ventricle size (Hami et al., 2011). In several mutants, such as *spaw* (Long et al., 2003; Noël et al., 2013) or *mom*, *boz, flh* and *ntl*, which disrupt the notochord (Chen et al., 1997), the directions of cardiac jogging and looping can be uncoupled, supporting the hypothesis that these two events are driven by distinct mechanisms.

In summary, live-imaging approaches in zebrafish have revealed that heart jogging is driven by intrinsic mechanisms (i.e. the asymmetric behaviour of myocardial cells), and genetic evidence is also consistent with intrinsic mechanisms of heart looping, generating a flat-S-shaped tube. Understanding whether extrinsic mechanisms also play a role will require 3D reconstructions of heart shape and analyses of cardiac precursor cells, which express the left determinant Nodal. In this animal model, the processes of jogging and looping are prone to errors, with 2-10% of wild-type animals displaying an aberrant orientation (Chen et al., 1997; Juan et al., 2018), thus indicating a lack of robustness. Another feature of the zebrafish heart, is the number of cardiac chambers – a single atrium and a single ventricle – thus underlying a single blood circulation.

Heart looping in the chick

Amniote models of heart morphogenesis are more relevant to model congenital heart defects, because of their four-chambered structure underlying a double blood circulation, as in humans. Owing to its accessibility, the avian embryo has proved to be a useful model; indeed, the sequence of morphological changes occurring at the looping stage was carefully observed and described by early embryologists (His, 1868; Patten, 1922). During avian development, a straight and bilaterally symmetrical heart tube forms at Hamburger and Hamilton (HH) stage 9, via fusion of the bilateral heart fields (Fig. 5). From HH10 to HH12, the primitive ventricular region bends ventrally and simultaneously rotates to the right by 90° (de la Cruz et al., 1989), taking on a C shape. The dorsal attachment of the tube, the dorsal mesocardium (see Glossary, Box 1), breaks down during

Development (2018) 145, dev162776. doi:10.1242/dev.162776

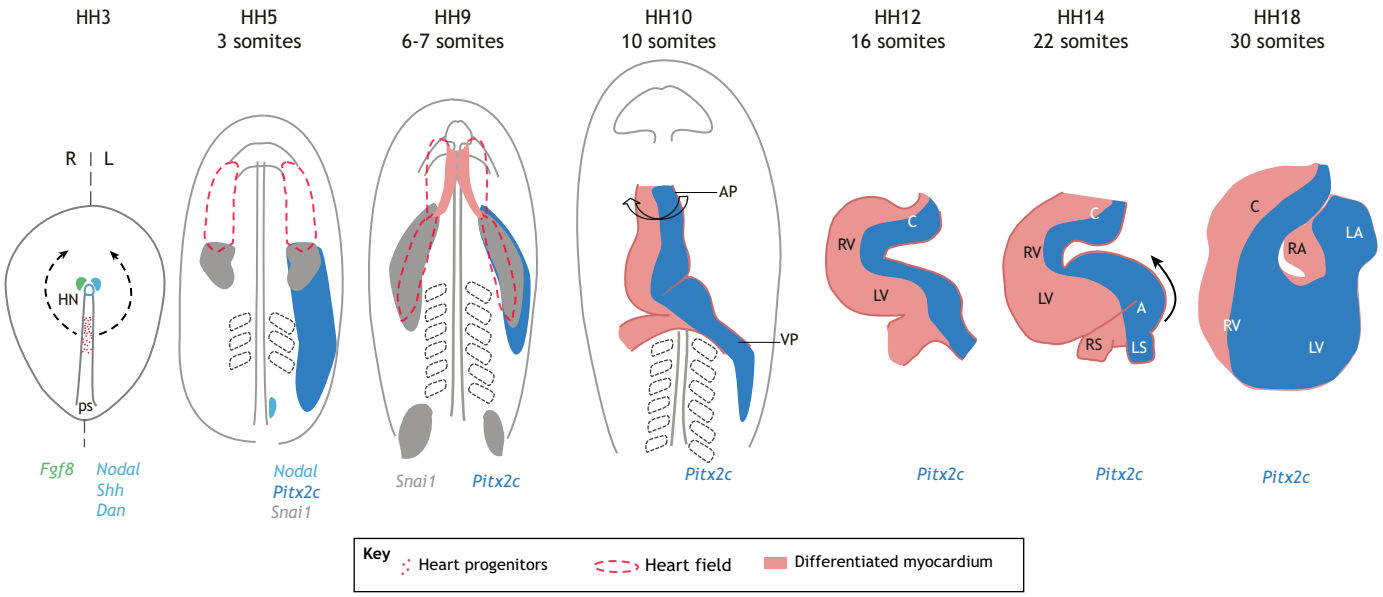

Fig. 5. Left-right asymmetric patterning and looping of the heart in the chick. In the chick, asymmetric gene expression (e.g. *Fgf8* and *Nodal*) is first seen at HH3 in the left-right organiser (which is termed Hensen's Node, HN) and then in the lateral plate mesoderm, with *Pitx2c* (blue) on the left at HH5 and higher levels of *Snai1* (grey) on the right at HH9. Heart precursor cells, which migrate anteriorly (dotted arrows) on either side of the primitive streak (ps), have been traced in two bilateral heart fields (red dotted line, HH5), which fuse to form a straight heart tube (red, HH9). From HH10, the tube bends on the right (curved arrow), thus acquiring a C-shape (HH12). Convergence of the arterial (AP) and venous (VP) poles starts at HH14 (arrow), resulting in an apparent S-shaped heart tube (HH18). A, atrium; C, conus; LA, left atrium; LS, left sinus venosus; LV, left ventricle; RA, right atrium; RS, right sinus venosus; RV, right ventricle.

this period, approximately between the 12- to 18-somite stages (Linask et al., 2005). Between HH9 and HH18, the looping process occurs and lasts about 2 days, during which time the total length of the heart tube increases 4.5-fold, from 0.6 mm to 2.7 mm (Patten, 1922). At the same time, the entire embryo undergoes a rightward axial rotation by 90° (see Fujinaga, 1997), which in some cases can be uncoupled from heart looping (Levin et al., 1997). From HH14 to HH18, the primitive outflow tract converges towards the atria, while the primitive ventricle is displaced posterior to the atria, thus forming a helix referred to as 'S-shaped loop' (Männer et al., 1993; Patten, 1922; Waldo et al., 2005). Later rotation of the outflow tract results in the helical arrangement of the aorta and pulmonary trunk, and the wedging of the aorta between the atrio-ventricular valves (Thompson et al., 1987).

Initial observations suggested that intrinsic factors are important for cardiac looping in the avian embryo. Hearts explanted from embryos before the onset of looping, and cultured for 24 h, were found to curve *in vitro* (Manning and McLachlan, 1990). However, quantification of the degree of looping was not carried out, and the final shape adopted by these hearts is more compatible with a ventral bending event rather than complete helical looping (Latacha et al., 2005). In addition, hearts isolated at the C-shape stage did not loop further (Ramasubramanian et al., 2013). Using a different approach, perturbation of the actin cytoskeleton locally, on the caudal right side of the straight heart, was shown to reverse looping direction (Itasaki et al., 1991), again supporting intrinsic mechanisms. However, this was questioned by further experiments using alternative culture conditions (Voronov et al., 2004), and showing that actin polymerization is required only for the initial ventral bending process rather than for the complete helical loop (Latacha et al., 2005). Another intrinsic factor, myocardial contractility, was ruled out based on the lack of effect of myosin inhibitors on heart looping (Rémond et al., 2006). Again, little intercalation between cells of the linear heart tube was detected, after radioactive or dye labelling in the left and right halves (Campione et al., 2001; Stalsberg, 1969). Asymmetries in cell growth (Manasek et al., 1972) or orientations of the actin cytoskeleton (Itasaki et al., 1991) have been observed in the heart tube, although whether these represent significant intrinsic factors for heart looping remains to be demonstrated.

In contrast, a number of studies have uncovered how extrinsic mechanisms can contribute to avian asymmetric heart morphogenesis. Early embryologists, for example, noticed mechanical constraints on the heart tube caused by its attachments at the poles and dorsally, and by its confinement in the pericardial cavity. They suggested a process of 'mechanical compulsion' (His, 1868; Patten, 1922), which was later renamed as the 'buckling hypothesis' (Bayraktar and Männer, 2014). More recent observations also support extrinsic mechanisms for heart looping. Quantitative reconstructions of BrdU labelling prior to looping show that cells in the early heart tube, before HH12, proliferate very slowly, in contrast to precursor cells, particularly at the posterior end (Soufan et al., 2006). This indicates that elongation of the heart tube involves the ingression of precursor cells. Cell-labelling approaches further reveal a mechanism of convergence-extension, similar to that driving the elongation of the foregut, which occurs at the same time (Kidokoro et al., 2018). The ingression of heart precursor cells occurs at both poles (de la Cruz et al., 1977), however with distinct outcomes. Ablation of the caudal part of the tube does not prevent the remaining tube to undergo rightward rotation, whereas ablation of the cranial part impairs the rotation of the tube, as well as the intensity of the deformation at the venous pole (Kidokoro et al., 2008), suggesting that asymmetries from both poles are important for heart looping. Indeed, a leftward displacement of the venous pole follows the rightward rotation of the arterial pole (Kidokoro et al., 2008). Computer simulations indicate that such increased deformation of the left atrial region could initiate the rightward rotation, but that external forces are required for completion of looping (Voronov et al., 2004). Physical experiments, with rubber tubes, and computer simulations have shown that extrinsic forces, applied to the two extremities of the tube so that they rotate in opposite directions, are

Development (2018) 145, dev162776. doi:10.1242/dev.162776

sufficient to produce the observed helical looping (Männer, 2004; Voronov et al., 2004). An asymmetric behaviour of cardiac precursor cells was shown by BrdU labelling, so that left precursor cells at the beginning of looping (HH12) proliferate more (Linask et al., 2005) and this correlates with a higher contribution of left cells to the caudal tube at this stage (Stalsberg, 1969). The correlation between proliferation and looping direction is retained upon treatment at HH9 with an inhibitor of matrix metalloproteinases (MMPs), which can invert the direction of heart looping, whereas higher proliferation is on the right side. Treatment with another modifier of the ECM, heparanase, which cleaves the polysaccharide chain of glycosaminoglycans that are normally found in the left heart field, alters looping direction (Yue et al., 2004), potentially via effects on cell recruitment. The heart field is exhausted after completion of heart looping at HH22 (de la Cruz et al., 1977; Waldo et al., 2001).

Mechanical constraints from either the envelope that surrounds the heart or the dorsal mesocardial attachment have also been investigated. A recent physical model, wherein a rubber tube grows within a hemispherical glass cavity, was shown to reproduce a helical shape, the sidedness of the helix being determined by a slight shift at one end (Bayraktar and Männer, 2014). However, cutting the splanchnopleure over the heart before looping only delays the rightward rotation of the heart tube (Nerurkar et al., 2006), thus limiting the role of this confinement to the caudal displacement of the ventricles (Ramasubramanian et al., 2013). Treatment with an MMP inhibitor before looping at HH10-11, or overexpression of VEGF in the quail embryo, prevents breakdown of the dorsal mesocardium, and leads to incomplete heart looping (Linask et al., 2005). The dorsal mesocardium may thus modulate buckling of the heart tube, as shown in the mouse (Le Garrec et al., 2017; discussed below), or, based on its own left-right asymmetries (Linask et al., 2005, 2003), may contribute to the oriented deformation, as shown in the gut tube (Davis et al., 2008).

The molecular pathway initiating left-right patterning has been well characterised in the chick embryo (Fig. 5) and shown to control the sidedness of heart looping (Levin et al., 1995; Logan et al., 1998). Downstream of the left determinant Nodal, the transcription factor Pitx2c was found to be expressed specifically in the left LPM, then in the left half of the heart tube at HH12 and, finally, in the ventral aspect of the heart, as well as in the entire left atrium at HH16 (Campione et al., 2001). Ectopic expression or downregulation of *Pitx2c* affects the direction of heart looping (Yu et al., 2001). This is potentially mediated by asymmetric expression of the non-muscle myosin Myh10 (flectin), downstream of Pitx2c (Linask et al., 2002). The transcription factor snail 1 (Snai1), which is a repressor of *Pitx2*, is expressed at slightly higher levels in the right LPM (Isaac et al., 1997), upon inhibition by Nodal on the left side (Patel et al., 1999), and is required for the direction of heart looping. In addition, a Bmp right-determining pathway controls expression of the transcription factor Prrx1, which is required for the direction of heart looping (Ocaña et al., 2017).

In summary, studies in the chick have led to the conclusion that the behaviour of cells inside the heart tube (i.e. intrinsic mechanisms) underlie the initial ventral bending, whereas the looping per se is mostly driven by extrinsic forces. Such forces, which may arise from mechanical constraints, are regulated in time and space (left-right), and control what is essentially a buckling mechanism, as hinted at by early embryologists. Notably, heart looping in avian embryos is a robust process, oriented rightward in 97% of control embryos (Hoyle et al., 1992). Although right determinants, in addition to the left determinant Nodal, have been identified, the dissection of the molecular cascade underlying heart looping in the chick embryo remains limited owing to the restricted array of genetic tools available for this model system.

Left-right asymmetric heart morphogenesis in the mouse

The efficient genetic tools available in the mouse model have been essential for dissecting the mechanisms and tracking specific cell populations underlying morphogenesis of the four-chambered heart. In the mouse, cardiac precursors first differentiate at the cardiac crescent stage (E8.5c, Fig. 6A), as recently analysed by time-lapse imaging (Ivanovitch et al., 2017). The right and left heart fields, which initially bulge at E8.5d, fuse to form a heart tube and at E8.5f the right ventricular region lies cranially to the primitive left ventricle (Zaffran et al., 2004). Although the shape of the heart tube looks bilaterally symmetrical from a ventral point of view, a rightward rotation of the arterial pole, by 25°, has been detected from 3D reconstructions of the heart (Le Garrec et al., 2017). This, in addition to the leftward displacement of the venous pole, then results in a rightward tilt of the tube at E8.5 g, which is the first external sign of left-right asymmetry (Biben and Harvey, 1997). Looping progresses, while the tube axis extends by addition of precursor cells at the arterial and venous pole (Domínguez et al., 2012; Kelly et al., 2001) and while the dorsal mesocardium breaks down (Le Garrec et al., 2017). At E8.5j, the heart tube has acquired a helical shape in which the right ventricle has been repositioned on the right of the left ventricle. Between E8.5e and E8.5j (Fig. 6A), heart looping occurs within about 12 h, during which time the length of the tube increases more than fourfold, from 180 to 800 µm (Le Garrec et al., 2017) and from 700 to 3000 cells (de Boer et al., 2012). Concomitant with heart looping, the entire embryo rotates rightward, by 180°, along its antero-posterior axis (see Fujinaga, 1997). This is a process referred to as embryo turning, during which the ventral side of the embryo, initially outside the yolk sac, is internalised and flexed. In experimental conditions, the direction of embryo turning can be uncoupled from that of heart looping (McCarthy and Brown, 1998; Przemeck et al., 2003), suggesting that the two mechanisms operate in parallel. After the completion of heart looping, the tube poles converge along the cranio-caudal axis, such that the outflow tract is positioned above the atria at E10.5. Transgenic markers have illustrated the rotation of the outflow tract from E9.5 (Bajolle et al., 2006), when the heart field is exhausted (Sun et al., 2007), underlying the spiralling of the aorta and pulmonary trunk.

Cell-tracing approaches have been used to map the contributions of left/right precursor cells (Fig. 6B). This is facilitated by the coherent growth of the myocardium within the tube (Meilhac et al., 2003), which limits mixing between left and right cells. Cell-labelling experiments have shown that left and right precursors contribute to the superior and inferior atrio-ventricular canal, respectively, with right cells contributing to the ventral left atrium in addition to the right atrium of the looped heart (Domínguez et al., 2012). Expression of the left marker *Pitx2c* largely follows this pattern at E9.5, with higher expression in the inner curvature, including in the atrio-ventricular canal and left atrium, but also in the outflow tract and right ventricle, and with a minor contribution to the inner curvature of the left ventricle (Campione et al., 1999; Furtado et al., 2011). Clonal analyses have shown that later, in the fetal E14.5 heart, the myocardium at the base of the aorta and pulmonary artery is related to right and left head skeletal muscles, respectively (Lescroart et al., 2010). In addition, the right superior caval vein was shown to be clonally related to the right atrium, whereas the left superior caval vein, the pulmonary vein and the pulmonary trunk are from the same lineage as the left atrium (Lescroart et al., 2012). How left-right signalling affects heart

Development (2018) 145, dev162776. doi:10.1242/dev.162776

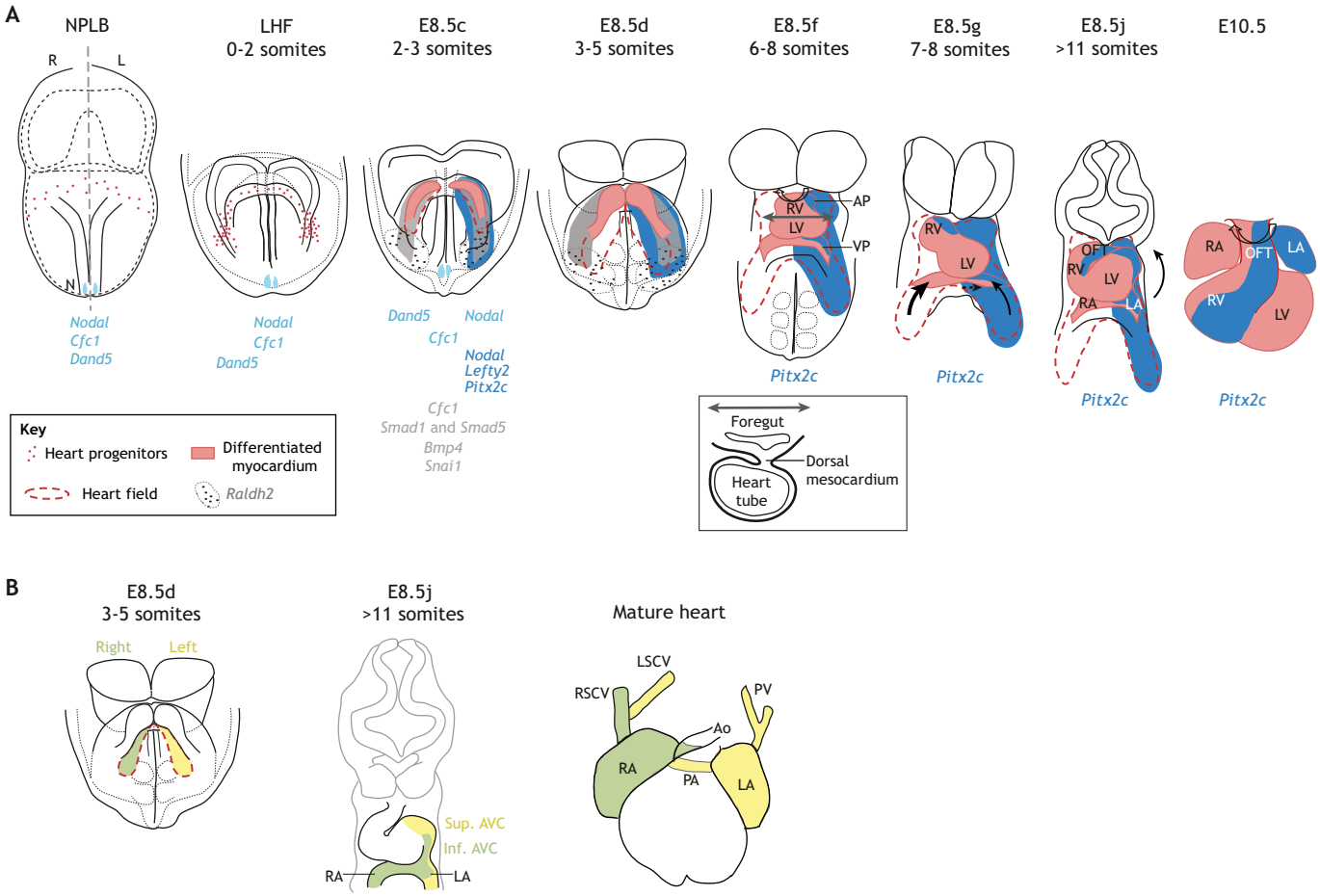

Fig. 6. Left-right asymmetric patterning and looping of the heart in the mouse. (A) In the mouse, asymmetric gene expression is initiated in the node (N) from the late headfold (LHF) stage at E7.5 with *Dand5* showing slightly higher levels on the right. In the LPM, asymmetric expression of components of the Nodal pathway (blue) is detected at E8.5c,d, and maintained later only for *Pitx2c*, whereas *Cfc1*, *Snai1*, *Raldh2* or components of the Bmp signalling pathway, are expressed symmetrically (grey). Cardiomyocytes first differentiate in the cardiac crescent stage (E8.5c). At E8.5f, the heart tube (red) is straight, the right ventricle (RV) lying cranially to the left ventricle (LV). The dorsal mesocardium has not yet started to break down (see lower diagram, presenting a section at the level of the double-headed arrow). Rotation of the arterial pole is indicated by a curved arrow. From E8.5g, the right ventricle is progressively repositioned on the right side. Asymmetric ingression of heart precursors at the venous pole is indicated by arrows. The leftward shift of the venous pole is represented by a dotted arrow. The typical helical shape of the looped heart tube is visible at E8.5j. At E10.5, the arterial and venous poles, which were initially anterior and posterior, have converged (arrow at E8.5j). Rotation of the outflow tract (OFT) continues (curved arrow, E10.5). (B) Results from lineages and cell-labelling experiments are schematised, showing the specific contribution of the right (green) and left (yellow) second heart field to the looped and mature heart. Ao, aorta; Inf. AVC, inferior atrio-ventricular canal; L, left; LA, left atrium; LSCV, left superior caval vein; LV, left ventricle; NPLB, neural plate late bud stage; OFT, outflow tract; PA, pulmonary artery; PV, pulmonary veins; R, right; RA, right atrium; RSCV, right superior caval vein; RV, right ventricle; Sup. AVC, superior atrio-ventricular canal.

precursor cell deployment remains an unresolved issue, as no cell tracing has been performed in mutant backgrounds.

Analysis of the behaviour of cardiomyocytes, within the heart tube, is relevant to potential intrinsic mechanisms of heart looping. Cardiomyocytes proliferate with regionalised differences during looping, with higher growth rates occurring in the outer curvature of the ventricles (de Boer et al., 2012). However, it remains unclear whether this is required for only cardiac chamber expansion or is also important for heart looping. In keeping with a potential role of oriented cell behaviour, myocardial growth was shown to be oriented (Meilhac et al., 2004; Le Garrec et al., 2013), and components of the non-canonical Wnt/PCP pathway, such as Wnt5a, Wnt11, Vangl2 or the effector Rac1, are expressed in the myocardium (Cohen et al., 2012; Leung et al., 2014; Ramsbottom et al., 2014). However, their polarity remains unknown, as does the requirement of an oriented cell behaviour for mouse heart looping. It is also not clear whether such intrinsic mechanisms of heart looping depend on left-right signalling factors. Nodal is transiently expressed in heart precursor cells but is turned off within the heart tube (Vincent et al., 2004). The Nodal target *Pitx2c*, which is asymmetrically expressed in the heart tube (Campione et al., 1999; Furtado et al., 2011), is dispensable for heart looping direction (Lu et al., 1999), and the deletion of *Pitx2c* specifically in cardiomyocytes does not impair heart looping (Ammirabile et al., 2012), thus ruling out a role of this gene in intrinsic regulation of heart looping. Expression of the non-muscle myosin Myh10 in the heart tube is decreased in *Nodal* mutants, raising the possibility that the actomyosin cytoskeleton may play a role for completion of heart looping (Lu et al., 2008). Components of the ECM (fibronectin), or factors interacting with it (Itga5), are also required for cardiac looping (Mittal et al., 2013; Pulina et al., 2011), but whether they are required within the heart tube or in precursor cells, and thus for intrinsic or extrinsic mechanisms, remains an unresolved issue. Explant approaches that can be used to delineate the contribution of such intrinsic mechanisms during heart looping in mice are currently lacking.

Development (2018) 145, dev162776. doi:10.1242/dev.162776

Analyses of the mechanical constraints present during heart growth, coupled to computer modelling, rather suggest that heart looping in the mouse follows an extrinsic mechanism (Le Garrec et al., 2017). In developing mouse embryos, the distance between the cardiac poles is fixed, while the cardiac tube elongates, supporting a buckling mechanism, as suggested in the chick model. Computer modelling and analyses of *Shh* mutants show that breakdown of the dorsal mesocardium modulates the intensity of the buckling, whereas small left-right asymmetries at the poles of the heart are sufficient to bias the buckling direction. These asymmetries, a rightward rotation and an asymmetric cell ingression, identified at the arterial and venous poles, respectively, are sequential and opposite, and thus can generate a helical shape in computer simulations. This model of looping functions as an asymmetry generator that is specific to the heart and is able to amplify variations in left-right patterning (Le Garrec et al., 2017). Such an extrinsic mechanism of heart looping is compatible with the observation that left-right patterning occurs in heart precursors, rather than within the heart tube. In the left LPM, which includes heart precursors, the main asymmetric determinant, Nodal, activates the transcription of itself, *Lefty2* and *Pitx2c*. Lefty2, in turn, which acts as a Nodal antagonist, establishes a negative-feedback loop that limits Nodal signalling to a short time window of a few hours (Meno et al., 2001), until E8.5e (Fig. 6). As a consequence, *Lefty2* is downregulated at E8.5f (Fig. 6), which terminates Nodal signalling in heart precursors. Blood flow is another potential extrinsic factor of heart morphogenesis. However, it is progressively established during cardiac looping (Nishii and Shibata, 2006), and thus is unlikely to play an early role in determining heart shape. Supporting this, the hearts of *Ncx1* mutants, in which myocardium contraction is absent, can still loop (Koushik et al., 2001).

In line with the buckling model, growth and elongation of the heart tube has been demonstrated to be essential for heart looping. When the transcription factors Isl1, Mef2c, Nkx2-5, Tbx3, Tbx5 or Tbx20 (Bruneau et al., 2001; Cai et al., 2003; Lin et al., 1997; Lyons et al., 1995; Ribeiro et al., 2007; Stennard et al., 2005), which are required for cardiomyocyte differentiation, are depleted, the heart tube is smaller, owing to defective cell ingression, and does not loop (Table 1). Another determinant of cell ingression underlying the elongation of the heart tube is the Wnt/PCP pathway. Indeed, the second heart field, lying in the dorsal pericardial wall, is organised as an epithelium (Francou et al., 2014), in which core components of the Wnt/PCP pathway, such as Wnt5, Vangl2, Prickle1 and Dvl, and the effector Myh10 are expressed (Gibbs et al., 2016; Ramsbottom et al., 2014; Sinha et al., 2012). Disruption of the PCP pathway results in incomplete heart looping, as if arrested at E8.5i (Fig. 6), and a shorter outflow tract (Gibbs et al., 2016; Henderson et al., 2001; Li et al., 2016; Phillips et al., 2007; Ramsbottom et al., 2014; Zhou et al., 2007). This is associated with a disorganisation of the second heart field, including abnormal cell morphology, adhesion and polarity, defective actin organization and premature cell differentiation (Gibbs et al., 2016; Leung et al., 2014; Li et al., 2016; Ramsbottom et al., 2014; Sinha et al., 2015). It was thus proposed that the Wnt/PCP pathway controls convergence-extension of heart precursors for their ingression into the arterial pole (Sinha et al., 2015). This is consistent with the observed fragmentation of labelled myocardial clones along the heart tube axis (Meilhac et al., 2003).

Table 1. List of mouse mutants with incomplete heart looping

	Mutant description	Stage	Heart phenotype	Reference
Nodal pathway	*Pitx2*$^{null/null}$	E9.5	Incomplete rightward looping	MGI:2384494, Lin et al. (1999)
		E10.5	Hypoplastic RV, enlarged LA	MGI:2136268, Lu et al. (1999), MGI:1857880, Kitamura et al. (1999)
Hedgehog pathway	*Shh*$^{null/null}$	E9.5	Incomplete rightward or ventral looping with persistent dorsal mesocardium	MGI:5440762, Le Garrec et al. (2017) MGI:1857796, Tsukui et al. (1999)
		E10.5	Incomplete looping	Hildreth et al. (2009)
PCP pathway	*Wnt5a*$^{null/null}$	E9.5	Incomplete rightward looping (~E8.5i)	MGI:1857617, Sinha et al. (2012; 2015)
	Wnt5a gain of function		Incomplete looping (~E8.5h), shortened OFT	Li et al. (2016)
	Wnt11^{null}	E9.5	Incomplete looping, shortened OFT	MGI:2665014, Zhou et al. (2007)
	Vangl2^{Lp}	E8.5, E9.5	Incomplete rightward looping (~E8.5i)	MGI:1857642, Henderson et al. (2001), Rambsottom et al. (2014)
	Scrib^{Crc}	E9.5, E10.5	Incomplete rightward looping (~E8.5i)	MGI:1889322, Phillips et al. (2007)
	Dvl1$^{null/null}$;*Dvl2*$^{null/null}$	E9.5	Incomplete rightward looping (~E8.5i)	MGI:2137230, Sinha et al. (2012)
	Dvl2$^{null/null}$	E10.5	Shortened OFT	MGI:2429760, Kioussi et al. (2002)
Other genes	*Fn*$^{null/null}$	E9.5	Incomplete rightward looping	MGI:1857170, Pulina et al. (2011), Mittal et al. (2013)
	Itga5$^{null/null}$	E9.5	Incomplete rightward looping (~E8.5g)	MGI:1857207, Mittal et al. (2013)
	Cdh2$^{fl/fl}$;*Mef2cAHF-Cre*	E9.5	Incomplete rightward looping, shortened OFT and hypoplastic RV	MGI:3522469, Soh et al. (2014)
	Tbx3$^{neo/neo}$	E9.5	Incomplete rightward looping (~E8.5h)	MGI:3769504, Ribeiro et al. (2007)
	Isl1$^{null/null}$	E8.5	Smaller and straight tube	MGI:2447758, Cai et al. (2003)
		E9.5	Lack of OFT and RV	
	Mef2c$^{null/null}$	E9	Smaller and straight tube, lack of OFT and RV	MGI:1857491, Lin et al. (1997)
	Nkx2-5$^{null/null}$	E9, E9.5	Smaller and straight tube	MGI:3655239, Lyons et al. (1995), Prall et al. (2007)
	Tbx20$^{null/null}$	E9, E9.25	Smaller and straight tube	MGI:3579836, Stennard et al. (2005)
			Lack of OFT	
	Tbx5$^{null/null}$	E9.5	Smaller and straight tube, hypoplastic LV and inflow	MGI:2387851, Bruneau et al. (2001)

OFT, outflow tract; LA, left atrium; LV, left ventricle; RV, right ventricle.

Development (2018) 145, dev162776. doi:10.1242/dev.162776

The second heart field, which provides cells for the elongation of the heart tube, is not only patterned along the left-right axis, but also along the antero-posterior axis. Several observations indicate that heart looping might integrate signals related to antero-posterior patterning. Anterior and posterior domains of the second heart field are characterised by distinct derivatives (Lescroart et al., 2010, 2012) and differential gene expression at E9.5 (Francou et al., 2014; Rana et al., 2014). This patterning is potentially already established at the time of heart looping (E8.5), as opposite left-right asymmetries are observed at the anterior (arterial) and posterior (venous) poles of the heart, as well as distinct antero/posterior kinetics of dorsal mesocardium breakdown (Le Garrec et al., 2017). Moreover, retinoic acid signalling, which is a key regulator of antero-posterior patterning of heart precursors (Hochgreb et al., 2003), appears to regulate heart looping; mice lacking the RA-synthesizing enzyme Raldh2 exhibit impaired heart looping, despite normal left-right patterning (Niederreither et al., 2001; Ryckebusch et al., 2008). However, the mechanism underlying looping defects in these mutants remains unclear; it may relate to the failure of dorsal mesocardium breakdown or to the posterior expansion of anterior markers of the second heart field, which are associated with impaired inflow and outflow development.

Although the studies discussed above have characterised several types of asymmetries in cardiac tissues, it remains unclear how the molecular left-right patterning established in the early embryo is translated to heart precursors and regulates heart-specific asymmetries. Malformation (e.g. Krebs et al., 2003) or dysfunction (e.g. Nonaka et al., 1998) of the left-right embryonic organiser impairs the direction of heart looping, which is often described as a randomisation of looping direction, although the proportions of the categories (rightward, leftward or undetermined) are rarely equal. However, cells of the left-right organiser do not contribute to the heart. Insight into the essential role of left-right signalling within heart precursor cells (Table 2) comes from targeted deletion of the asymmetric enhancer (ASE) of *Nodal*, which is specific to the LPM and impairs heart looping (Norris et al., 2002). An asymmetric enhancer is also found in *Lefty2* and *Pitx2c*, and contains binding sites for the transcription factor Foxh1. Mouse genetic experiments showed that Foxh1 is required in the LPM for Nodal-activated gene transcription and the direction of heart looping (Yamamoto et al., 2003). This is also the case for the Nodal co-receptor Cfc1, which is bilaterally expressed in the LPM (Yan et al., 1999). However, the effectors of Nodal signalling within heart precursors remain unclear. *Pitx2c*, which is required for the completion of heart looping, but not for its direction (Lin et al., 1999; Lu et al., 1999), is expressed in the left second heart field, downstream of the cardiac transcription factors Tbx1 and Nkx2-5 (Nowotschin et al., 2006). It is required for asymmetric proliferation in the sinus venosus (hindering proliferation on the left) and represses right atrial identity (Galli et al., 2008). However, whether Pitx2c or another Nodal effector controls other asymmetric cell behaviours, such as proliferation in the second heart field or cell ingression at the venous pole, as observed at E8.5 (Le Garrec et al., 2017), is an unresolved issue. The relative contribution of right-sided signals also remains unclear. The right identity of the LPM could be defined by default as not being 'left', as no signal exclusive to the right side has been uncovered. Evidence of potential 'rightness' signals comes from the study of Bmp signalling, which competes with that of Nodal for the common effector Smad4. In absence of the Bmp effectors Smad1/5, *Nodal* is expressed

Table 2. List of mouse mutants with an abnormal direction of heart looping

	Mutation description	Nodal pathway in LLPM	Stage	Looping direction defects	MGI number and reference
Nodal pathway	*Nodal*$^{\Delta 600/-}$	Absent	E9	No direction	MGI:2181581, Norris et al. (2002)
	Nodal$^{\Delta/fl}$; *EIIa*$^{Cre/+}$	Absent	E8.5	50%/50% normal/reversed	MGI:2158730, Lowe et al. (2001)
	Foxh1$^{null/null}$	Absent	E9.5	No direction 90% (*n*=140)	MGI:2179442, Von Both et al. (2004)
	Foxh1$^{fl/null}$; *Lefty2-3.0-Cre*			Normal (19/41) No direction (7/41) Reversed (15/41)	MGI:2387775, Yamamoto et al. (2003)
	Cfc1$^{null/null}$	Absent	E8.5	Randomised (21/45)	MGI:2179530, Yan et al. (1999)
	Furin$^{null/null}$	Left	E8.5, E9.5	No direction or no heart tube	MGI:1857604, Roebroek et al. (1998)
BMP pathway	*Smad1*$^{null/null}$	Caudal bilateral	E9.5	Normal (13/43) Reversed (20/43) No direction (10/43)	MGI:2155484, Furtado et al. (2008)
	Smad1$^{fl/fl}$; *Mesp1*$^{Cre/+}$	Cranial bilateral		Normal (19/25)	
	Smad5$^{null/null}$	Bilateral or absent	E9.5	Straight OFT (6/17) Randomised direction of the OFT (9/17) No direction (2/17)	MGI:1857666, Chang et al. (2000)
	Bmp4$^{null/null}$	Absent	E8.5	Normal (3/7) No direction (4/7)	MGI:1857137, Fujiwara et al. (2002)
	pMes-loxSTOPlox-Noggin; *Nkx2-5*$^{Cre/+}$	na	E8.5, E9	No direction/reversed	Simmons et al. (2015)
	Chrd$^{null/null}$; *Nog*$^{null/null}$	Absent	E9	No direction/reversed	MGI:2157350, MGI:1862000, Mine et al. (2008)
	Snai1$^{fl/null}$; *Meox2-Cre*	Bilateral	E9.5	Normal (27/73) No direction (17/23) Reversed (29/73)	MGI:3617387, Murray and Gridley (2006)
Retinoic acid	*Raldh2*$^{null/null}$	na	E8.5, E9.5	No direction	MGI:2180721, Mic et al. (2002), MGI:1857891, Ryckebusch et al. (2008)
	RA loss of function	Absent	E9	Reversed 45%	Chazaud et al. (1999)
	RA gain of function	Bilateral		Reversed 40%	

fl, flox; LLPM, left lateral plate mesoderm; na, not available; OFT, outflow tract; RA, retinoic acid.
Signals from the lateral plate mesoderm are listed here. Mutants with malformation or dysfunction of the node, also associated with heart looping defects, are excluded.

Development (2018) 145, dev162776. doi:10.1242/dev.162776

bilaterally in the LPM and the direction of heart looping is compromised (Chang et al., 2000; Furtado et al., 2008). This indicates that Bmp signalling limits the availability of Smad4 in the right LPM (Furtado et al., 2008). Accordingly, invalidation of *Bmp4*, or of both the Bmp antagonists noggin (Nog) and chordin, or the ectopic left expression of *Nog*, impairs heart looping (Fujiwara et al., 2002; Mine et al., 2008; Simmons et al., 2015). Another potential right marker of the LPM is the transcription factor Snai1, which shows subtle and transient asymmetric expression in the LPM (Sefton et al., 1998). Inactivation of *Snai1* in the epiblast results in bilateral expression of *Nodal*, *Lefty2* and *Pitx2c*, and randomised heart looping direction (Murray and Gridley, 2006). In the future, it will be important to understand how these right determinants modulate cardiac cell behaviour.

In summary, the array of genetic tools available for studying the mouse model, including the possibility of targeting gene modifications to specific cell populations, has been instrumental in dissecting the mechanisms underlying the asymmetric morphogenesis of the four-chambered heart. These studies suggest that heart looping is mainly driven by extrinsic mechanisms, whereby the patterning of heart precursors is essential to bias tissue deformations. Intrinsic mechanisms of heart looping may provide additional modulations of shape, but remain to be demonstrated. Currently, the inaccessibility of the mouse embryo (i.e. its *in utero* development) limits the analyses of cell behaviour by live imaging. However, advances in imaging technologies together with the development of tools that can quantify shape changes in 3D raise the possibility of understanding many more aspects of heart looping than only its direction. Given the anatomical similarities between the mouse and human hearts, the mouse model has proved to be useful for understanding heart malformations. Indeed, mouse mutants with abnormal heart looping later develop several types of congenital heart defects, which correspond to impaired left-right identity or impaired position of cardiac segments, misconnections between them or septation defects (Table 3). An unresolved issue is understanding how specific aspects of heart looping determine specific types of cardiac segment anomalies. The left-right identity of the inflow of the heart is established independently of looping directionality. Left isomerism (see Glossary, Box 1) of the atria can be associated with rightward looping in *Lefty2*, *Shh* or *Smad1* mutants, where Nodal is bilaterally expressed (Furtado et al., 2008; Hildreth et al., 2009; Meno et al., 2001), whereas right atrial isomerism is observed in *Cfc1* mutants (Yan et al., 1999), in which abrogation of Nodal signalling randomises heart looping direction, and thus is potentially associated with leftward looping. Mouse mutants with randomised or incomplete heart looping also present anomalies of the outflow tract, i.e. malposition of the great arteries, such as transposition or double outlet right ventricle. Whether this is a direct consequence of heart-looping anomalies or is associated with defective rotation of the outflow tract, which persists after heart looping, remains to be investigated. Correlations between the embryonic loop shape and defects in the structure of the mature heart are currently limited by the variability of mutant phenotypes, as exemplified by the 'randomisation' of looping direction.

The evolution of heart looping

The three vertebrate models discussed above, which diverged about 400 million years ago, show striking similarities with regard to their spatio-temporal dynamics of asymmetric heart morphogenesis. In all three cases, the heart tube forms from the fusion of bilateral fields of cardiac precursors, coinciding with the time of cardiomyocyte differentiation. Inside the tube, cardiomyocytes proliferate at a low rate and tube elongation largely arises from cell ingression, and potentially by a mechanism of convergence-extension, as demonstrated in the chick. Heart precursors are patterned along the antero-posterior and left-right embryonic axes. Conserved signalling pathways, such as the Nodal and Bmp pathways, are involved in patterning the heart fields. Left-right asymmetric gene expression precedes the progressive appearance of morphological asymmetries, with regionalisation at the arterial and venous poles. A rightward rotation occurs at the arterial poles in amniotes or in the disc in the fish, followed by a leftward displacement of the venous pole in the three species. The left determinant Nodal is expressed in the LPM, whereas its targets, such as *lefty*2 in the fish or *Pitx2c* in amniotes, are expressed within the heart tube. The initial left-right patterning is converted into a ventral-dorsal regionalisation, in keeping with the rotation of the tube/cone along its axis. In all three cases, heart looping coincides with the expansion of the cardiac chambers, raising the issue of whether these processes are linked.

Table 3. Spectrum of heart defects associated with abnormal looping in the mouse model

CHD	Associated genes	References
Malposition of the heart apex	*Cfc1*, *Foxh1*, *Nodal*	Yan et al. (1999), Yamamoto et al. (2003), Lowe et al. (2001), Norris et al. (2002),
DORV	*Dvl1/2*, *Fgf8*, *Foxh1*, *Nkx2-5*, *Pitx2c*, *Prickle1*, *Scrib*, *Vangl2*, *Wnt11*	Sinha et al. (2012), Frank et al. (2002), Yamamoto et al. (2003), Prall et al. (2007), Bajolle et al. (2006), Ai et al. (2006), Gibbs et al. (2016), Philips et al. (2007), Henderson et al. (2001), Zhou et al. (2007), van Vliet et al. (2017)
TGA	*Cfc1*, *Fgf8*, *Foxh1*, *Nodal*, *Pitx2c*, *Scrib*, *Wnt11*	Yan et al. (1999), Frank et al. (2002), Yamamoto et al. (2003), Lowe et al. (2001), Bajolle et al. (2006), Ai et al. (2006), Ammirabile et al. (2012), Philips et al. (2007), Zhou et al. (2007), van Vliet et al. (2017)
Left atrial isomerism	*Lefty1/2*, *Shh*, *Smad1*	Meno et al. (1998), Meno et al. (2001), Hildreth et al. (2009), Furtado et al. (2008), Yan et al. (1999)
Right atrial isomerism	*Foxh1*, *Pitx2*, *Cited2*, *Cfc1*	Yamamoto et al. (2003), Ammirabile et al. (2012), Bamforth et al. (2004), Yan et al. (1999)
Defective pulmonary vein return	*Fgf8*, *Pitx2*, *Shh*	Frank et al. (2002), Mommersteeg et al. (2007), Hildreth et al. (2009)
AVSD	*Rac1*, *Scrib*, *Shh*, *Tbx1*, *Wnt11*	Leung et al. (2014), Phillips et al. (2007), Hildreth et al. (2009), Rana et al. (2014), Zhou et al. (2007), van Vliet et al. (2017)
VSD	*Cfc1*, *Dvl1/2*, *Fgf8*, *Foxh1*, *Nkx2-5*, *Prickle1*, *Rac1*, *Vangl2*	Yan et al. (1999), Sinha et al. (2012), Frank et al. (2002), Yamamoto et al. (2003), Prall et al. (2007), Gibbs et al. (2016), Leung et al. (2014)

AVSD, atrioventricular septal defect; CHD, congenital heart defect observed at birth; DORV, double outlet right ventricle; TGA, transposition of the great arteries; VSD, ventricular septal defect.

Defects are considered here individually and potential association between them or with defects in other visceral organs, such as in the heterotaxy syndrome, is not presented, owing to incomplete descriptions in many mouse models.

Development (2018) 145, dev162776. doi:10.1242/dev.162776

The four-chambered heart includes another level of asymmetry than looping, with regard to the left/right identity of cardiac segments (atria, ventricles, great vessels). Although the zebrafish has a single atrium, recent analysis of the expression profile of meis2b has shown that the adult atrium is left/right regionalised (Guerra et al., 2018). However, the early expression of meis2b at the disc stage is posterior, not left, and thus it remains unclear how it relates to left-right patterning.

There are also significant differences between the three vertebrate models of asymmetric heart morphogenesis. In amniotes, heart looping occurs at the time of tube rotation and leftward displacement of the venous pole, whereas the process of heart looping in the fish, in which the tube acquires an S-shape, has been described as a second phase that can be uncoupled from the first. In amniotes, the second phase corresponds to the convergence of the tube poles, and in the chick is also referred to as the 'S-shaped loop' stage. Caution should therefore be taken regarding the confusing use of similar words, potentially masking different developmental processes. It will be important to measure the distance between the tube poles in the fish to assess whether a convergence process also occurs. Morphological analyses at adult stages in different species would suggest that convergence between the inflow and outflow of the heart is increased during vertebrate evolution (Simões-Costa et al., 2005). In the fish, the primitive heart is cone-shaped and circumferentially closed, which is very different to amniotes, where the tube initially fuses only ventrally. The dorsal attachment of the tube, by the dorsal mesocardium, breaks down progressively during heart looping, providing a mechanical constraint specific to amniotes. The heart tube in the fish, which telescopes out, displays free poles, as distinct from the fixed distance between the poles in amniotes during heart tube elongation. This corresponds to another mechanical constraint specific to amniotes, in keeping with the demonstration of intrinsic mechanisms that drive heart looping in the fish. The lack of buckling in the fish heart tube may therefore arise from differences in geometry, as well as in stiffness. The occurrence of buckling is given by Euler's formula, showing that the force above which buckling will occur is proportional to the stiffness of the tissue, but inversely proportional to the square of its effective length. Thus, for a tube half as long (comparing stages of 24 hpf in the fish and E8.5 g in the mouse, when the leftward displacement of the venous pole has occurred), the force needed for buckling would be four-fold higher. However, it can be noted that blood pressure is much lower in fishes compared with amniotes, which would suggest a lower stiffness of the myocardial wall, leading to uncontrolled buckling. It is therefore tempting to speculate that evolution has taken advantage of mechanical forces to produce a helical shape that intrinsic cell behaviours alone could only yield by processes that may be associated with a higher energetic cost. This would also explain why looping in the fish is less robust compared with that in amniotes. Between amniotes, there are variations in the mechanical constraints, as the heart tube is three-fold longer in the chick compared with mouse. Such increased confinement of the mouse heart tube within the pericardial cavity is in keeping with the shape of the mouse embryo, which develops as a cup-shape egg cylinder compared with the flat chick embryo. There are additional differences in cell behaviour between amniotes, such that left cells contribute more to the chick heart tube, as also reflected by the extent of the *Pitx2c* expression profile. The function of *Pitx2* is not well conserved, as it controls looping direction in the chick and not in the mouse. The evolutionary comparisons between animal models provide an illustration of the general concept that mechanistic variations that are also observed in the initial symmetry-breaking event in the left-right organiser (see Coutelis et al., 2014), may converge in similar outputs producing asymmetric heart morphogenesis. Finally, there are differences in the mature shape of the heart: in the fish it is a flat S shape, with a single atrium and ventricle driving a single blood circulation; in amniotes, a 3D helical shape is associated with a double blood circulatory system. Based on this, we propose that only the fully buckled helical shape is compatible with a stronger deformation underlying the precise alignment of four cardiac chambers.

Clinical relevance

In humans, laterality defects refer to a spectrum of developmental disorders resulting from anomalies in the establishment of left-right asymmetry (Lin et al., 2014). With a global prevalence of about 1/2000 (Table 4), they include simple or complex congenital heart defects, and are often associated with defects in other visceral organs, such as the lung, spleen, stomach, intestine, liver and pancreas. Dextrocardia is an example of an asymptomatic case in which the heart apex points to the right side of the thoracic cavity instead of the left (Fig. 7A,B). In situs inversus (see Glossary, Box 1), all visceral organs, not just the heart (Fig. 7C), are mirror-imaged compared with the normal situation (e.g. heart, spleen and

Table 4. Laterality defects in humans

Disease	Genetics	Prevalence	References
Isolated dextrocardia		1/36,000*	Bohun et al. (2007)
Situs inversus totalis	*ANKS3*, *CFAP52*/*53*, *CITED2*, *MMP21*, *NME7*, *NODAL*, *PKD1L1*	3/100,000	Lin et al. (2014) Orphanet
Primary ciliary dyskinesia with situs inversus	*ARMC4*, *C21ORF59*, *CCDC39*/*40*/*65*/*103*/*114*/*151*/*164*, *DNAAF1*/*2*/*3*, *DNAH5*/*11*, *DNAI1*/*2*, *DNAL1*, *DYX1C1*, *HEATR2*, *LRRC6*, *SPAG1*, *TXNDC3*, *ZYMND10*	1/32,000‡	Boon et al. (2014), Harrison et al. (2016) Kennedy et al. (2007),
Heterotaxy	*ACVR2B*, *CFAP52*/*53*, *CFC1*, *CRELD1*, *FGF12*, *FOXH1*, *FZD3*, *GALNT11*, *GDF1*, *LEFTY2*, *MED13L*, *MIR302F*, *MMP21*, *NIPBL*, *NKX2-5*, *NODAL*, *NPHP4*, *PPP4C*, *RBFOX1*, *SESN1*, *SHROOM3*, *TBX6*, *ZIC3*	8/100,000	Lin et al. (2014), Guimier et al. (2015), Hagen et al. (2016)
Transposition of the great arteries (TGA) (without heterotaxy)	*ACVR2B*, *CFC1*, *GDF1*, *LEFTY2*, *MYH6*, *MED13L*, *MKRN2*, *NAA15*, *NODAL*, *NPHP4*, *RAB10*, *SMAD2*, *ZIC3*	1/3500-5000	Martins and Castela (2008), Bouvagnet and de Bellaing (2016)
Congenitally corrected transposition of the great arteries (CCTGA)	Unknown	1/33,000	Wallis et al. (2011)

*Calculated from the incidence of dextrocardia and the percentage of cases (33%) with situs solitus (Bohun et al., 2007).
‡Calculated from the prevalence of PCD and the percentage (50%) of PCD cases with situs inversus (Harrison et al., 2016).

Development (2018) 145, dev162776. doi:10.1242/dev.162776

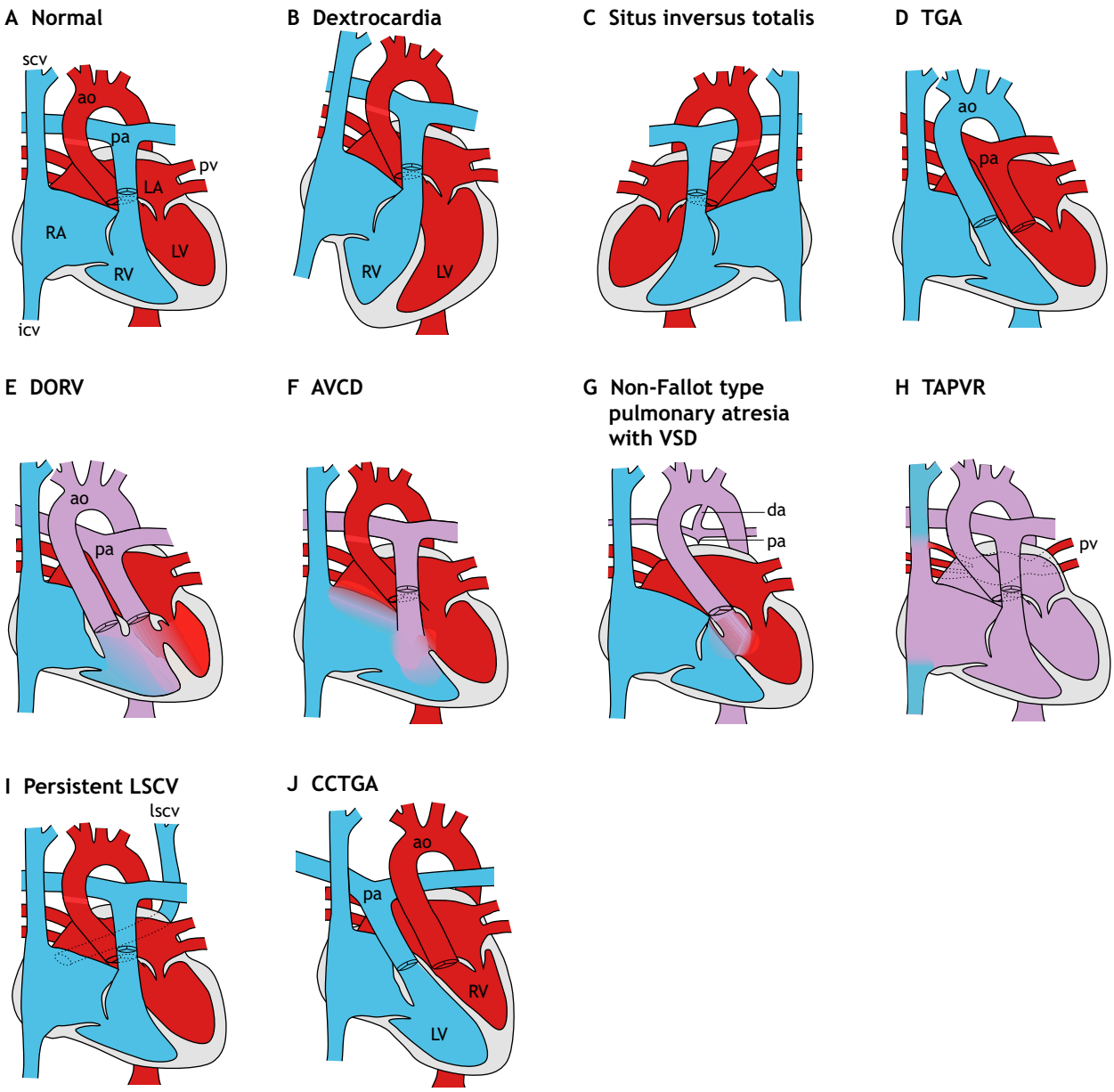

Fig. 7. Congenital heart defects associated with laterality defects. In the normal heart structure (A), the oxygenated (red) and carbonated (blue) bloods are confined to the left and right side of the heart, respectively. This is also the case in dextrocardia (B) but the apex of the heart points to the right side of the thoracic cavity instead of the left. (C) In situs inversus, the heart is mirror imaged. (D) In transposition of the great arteries (TGA), the positions of the pulmonary trunk and aorta are inverted. (E-I) Other defects observed in the heterotaxy syndrome. (E) In double outlet right ventricle (DORV), the two great arteries are positioned above the right ventricle. (F) In atrio-ventricular canal defects (AVCD), the atria are not septated (common atrium), the ventricles communicate and there is a single atrio-ventricular valve. (G) In non-Fallot type pulmonary atresia with ventricular septal defect (VSD), the pulmonary artery is not connected to a ventricle and the ductus arteriosus (da) is persistent. (H) In total anomalous pulmonary venous return (TAPVR), the pulmonary veins are connected to the caval veins and not to the left atrium. (I) In persistent left superior caval vein (LSCV), the embryonic left caval vein fails to regress. (J) In congenitally corrected transposition of the great arteries (CCTGA), the positions of the ventricles and great vessels are inverted. Many of these changes lead to reduced oxygenation of the blood (shown in purple). The left/right identity of cardiac segments is determined from anatomical features and therefore is independent of their position within the thoracic cavity. ao, aorta; icv, inferior caval vein; LA, left atrium; LV, left ventricle; pa, pulmonary artery; pv, pulmonary vein; RA, right atrium; RV, right ventricle; scv, superior caval vein.

stomach on the right; liver on the left). Situs inversus is most often associated with no (in 59% of cases) or simple (in 14% of cases) congenital heart defects (Lin et al., 2014). The most striking type of laterality defects, and the one that is the most severe, is heterotaxy syndrome. It corresponds to abnormal symmetry of the viscera (isomerism) and/or situs discordance between visceral organs (Van Praagh, 2006). In 90% of cases, it is associated with congenital heart defects, which are mainly (in 82% of cases) complex defects (Lin et al., 2014). Such defects include transposition of the great arteries (Fig. 7D), double outlet right ventricle (Fig. 7E), atrio-ventricular canal defects (Fig. 7F), pulmonary stenosis or atresia (Fig. 7G), anomalous pulmonary venous return (Fig. 7H), systemic venous anomalies (Fig. 7I), ventricular and atrial septal defects, single ventricle, and rhythm disorders (Jacobs et al., 2007; Lin et al., 2014; Mishra, 2015). Many of these defects, which can arise in combination, can have profound functional impacts, leading to

Development (2018) 145, dev162776. doi:10.1242/dev.162776

abnormal oxygen supply to the body or obstructed flow in/out of the heart. In 17.5% of cases of heterotaxy, the overall organ situs is symmetrical and right-sided (right isomerism), and this is more significantly associated with specific congenital heart defects such as total anomalous pulmonary venous return, complete atrio-ventricular canal defect, non-Fallot type pulmonary atresia, single ventricle, transposition of the great arteries and bilateral sinus nodes (Lin et al., 2014; Mishra, 2015). In another 18.5% of cases, the overall organ situs is symmetrical and left-sided (left isomerism), and this is more significantly associated with an interrupted inferior vena cava, a primum-type atrial septal defect and an absent sinus node. Mechanistically, the defects found in isomerism are relevant to the left/right origins of cardiac segments, as demonstrated in clonal analyses in the mouse (Lescroart et al., 2010, 2012): defects in pulmonary veins and the pulmonary trunk, which have a left origin, are associated with right isomerism, whereas interruption of the inferior caval vein, which has a right origin, is associated with left isomerism. The bilateralisation of the sinus node in right isomerism is consistent with the repression of its formation by the left marker *Pitx2* (Ammirabile et al., 2012). However, there is a significant overlap between the two categories of isomerism, so that cardiac features of each category can be found together in the same individual.

Genetically, heterotaxy is strongly associated with mutations in genes (e.g. *MMP21*, *ZIC3*) that are involved in the formation of the node, which is the left-right embryonic organiser in which lateral symmetry is first broken (Nonaka et al., 1998; Table 4). Mutations in ciliary genes (e.g. *CFAP52/54*, *NPHP4*), which are implicated in generating the leftward fluid flow in the node, and in components of the Nodal pathway (e.g. *ACVR2B*, *CFC1*, *FOXH1*, *GDF1*, *LEFTY2*, *NODAL*), which are a readout of the node function, may also be found in heterotaxy (Brennan et al., 2002). Heterotaxy syndrome is therefore associated with a randomisation of left-right patterning, with potential discordance between different anatomical structures. Situs inversus is associated with variations in genes that are similar to those affected in heterotaxy (Table 4), suggesting a continuous spectrum of defects. Situs inversus is also frequent in primary ciliary dyskinesia, which is caused by mutations in motile cilium genes (Harrison et al., 2016). Transposition of the great arteries (TGA), which is a defect found in heterotaxy, is also observed isolated in association with genetic variations common to heterotaxy (see Bouvagnet and de Bellaing, 2016; De Luca et al., 2010). This is a severe congenital heart defect in which the two blood circulations run in parallel, and thus systemic blood can no longer be oxygenated (Fig. 7D). This defect, which has to be repaired surgically, may result from defective rotation of the outflow tract, which is a rightward process (Bajolle et al., 2006). It is often associated with defective coronary stems, which normally emerge above the left and right leaflets of the aortic valve (Sithamparanathan et al., 2013). Congenitally corrected transposition of the great arteries (CCTGA) can also be classified as a laterality defect, on the basis of the recurrence of TGA in the same families (Digilio et al., 2001). It corresponds to an inverted position of the ventricles, combined with a transposition of the great vessels, thus maintaining a normal blood circulation (Fig. 7J). Despite the correct blood circulation, individuals with CCTGA are at a higher risk of cardiac insufficiency, because the structure of the right ventricle cannot support a systemic function. The inverted positions of the ventricles would suggest defective heart looping. However, the origin and genetics of CCTGA are currently unknown. Other genetic variations underlying laterality defects may be detected in genetic studies (see above) or genetic screens (Li et al., 2015) in the mouse, and in the expanding genetic analyses of individuals with congenital heart defects (e.g. Jin et al., 2017).

Conclusions and perspectives

As we have highlighted here, heart looping emerges as a fine morphogenetic process, integrating different patterning and signalling cues, and can no longer be reduced to a simple directional problem (rightward, leftward, undetermined direction). Although the diversity of heart loop shapes, as well as their frequency, observed in mutant animals remains poorly understood, the 3D reconstructions that have been developed using the mouse model open up novel avenues for increasing the level of resolution when comparing markers of asymmetry or when characterising mutant phenotypes. Such approaches will be essential to address the exquisite geometry of the heart loop and its spatio-temporal dynamics. Following on from the extensive studies on the initial symmetry-breaking events, a challenge for the future will be to address the effectors of left-right signals and how they modulate cardiac cell behaviour, which will reinforce the characterisation of the heart-specific generator of asymmetry. In addition, the link between heart looping and simultaneous events such as chamber ballooning, convergence of the inflow and outflow poles, or closure of the foregut, is still an unresolved issue that requires attention.

There is still much to be gained from parallel investigations in different animal models. These model comparisons are not only relevant for understanding the evolutionary conservation of the underlying mechanisms, but question their importance for a specific shape and function. However, it must be noted that pooling data acquired in different animal models, and using similar terminologies that might mask distinct mechanisms, is a potential source of confusion. Heart looping is not specific to species with a four-chambered heart and a double blood circulatory system. This might be linked to a functional advantage of looping with regard to increasing pumping efficiency, particularly at embryonic stages when the valves have not formed (Hiermeier and Männer, 2017). The looping mechanism appears to evolve from being a broadly intrinsic mechanism, in the case of fish, to a broadly extrinsic one in the case of amniotes. However, further work will be required to consolidate this view and test whether this reflects the requirement of a more efficient mechanism, provided by buckling, when looping becomes essential for a novel heart function, i.e. the establishment of a double blood circulatory system by the fine alignment of cardiac segments.

As laterality defects may affect several anatomical features, with randomised events, current analyses in mutant animals are often limited by fragmented analyses and insufficient quantifications. To fully exploit studies in animal models, it will therefore be important to develop standardised procedures for an exhaustive phenotyping of laterality defects, using clinical nomenclature. In the clinics, laterality defects, which together represent about 5% of congenital heart defects, are mainly associated with an early dysfunction of the left-right organiser, which also impacts the formation of other visceral organs. As studies in animal models indicate that left-right asymmetry of the heart is a multi-step process, it is possible that genetic variations in later determinants of the heart-specific generator of asymmetry, potentially downstream of the node, could cause congenital heart defects such as isolated segmental defects or discordance between cardiac segments. Deciphering the molecular cascade controlling asymmetric heart morphogenesis, beyond the left-right organiser, will be key in addressing this issue.

Acknowledgements

We thank D. Yelon, J. Vermot and L. Houyel for helpful comments on the manuscript.

Competing interests

The authors declare no competing or financial interests.

Funding
Work in the Meilhac lab is supported by core funding from the Institut *Imagine* and Institut Pasteur, and by a grant from the Agence Nationale de la Recherche [ANR-16-CE17-0006-03]. S.M.M. is a research scientist at the Institut National de la Santé et de la Recherche Médicale.

References

Ai, D., Liu, W., Ma, L., Dong, F., Lu, M.-F., Wang, D., Verzi, M. P., Cai, C., Gage, P. J., Evans, S. et al. (2006). Pitx2 regulates cardiac left-right asymmetry by patterning second cardiac lineage-derived myocardium. *Dev. Biol.* **296**, 437-449.

Ammirabile, G., Tessari, A., Pignataro, V., Szumska, D., Sutera Sardo, F., Benes, J., Jr, Balistreri, M., Bhattacharya, S., Sedmera, D. and Campione, M. (2012). Pitx2 confers left morphological, molecular, and functional identity to the sinus venosus myocardium. *Cardiovasc. Res.* **93**, 291-301.

Anderson, R., Spicer, D. and Loomba, R. (2018). Is an appreciation of isomerism the key to unlocking the mysteries of the cardiac findings in heterotaxy? *JCDD* **5**, 11-11.

Auman, H. J., Coleman, H., Riley, H. E., Olale, F., Tsai, H.-J. and Yelon, D. (2007). Functional modulation of cardiac form through regionally confined cell shape changes. *PLoS Biol.* **5**, e53-e12.

Bajolle, F., Zaffran, S., Kelly, R. G., Hadchouel, J., Bonnet, D., Brown, N. A. and Buckingham, M. E. (2006). Rotation of the myocardial wall of the outflow tract is implicated in the normal positioning of the great arteries. *Circ. Res.* **98**, 421-428.

Baker, K., Holtzman, N. G. and Burdine, R. D. (2008). Direct and indirect roles for Nodal signaling in two axis conversions during asymmetric morphogenesis of the zebrafish heart. *Proc. Natl. Acad. Sci. USA* **105**, 13924-13929.

Bamforth, S. D., Bragança, J., Farthing, C. R., Schneider, J. E., Broadbent, C., Michell, A. C., Clarke, K., Neubauer, S., Norris, D., Brown, N. A. et al. (2004). Cited2 controls left-right patterning and heart development through a Nodal-Pitx2c pathway. *Nat. Genet.* **36**, 1189-1196.

Bayraktar, M. and Männer, J. (2014). Cardiac looping may be driven by compressive loads resulting from unequal growth of the heart and pericardial cavity. Observations on a physical simulation model. *Front. Physiol.* **5**, 1-15.

Biben, C. and Harvey, R. P. (1997). Homeodomain factor Nkx2-5 controls left/right asymmetric expression of bHLH gene eHand during murine heart development. *Genes Dev.* **11**, 1357-1369.

Bisgrove, B. W., Essner, J. J. and Yost, J. (2000). Multiple pathways in the midline regulate concordant brain, heart and gut left-right asymmetry. *Development* **127**, 3567-3579.

Bohun, C. M., Potts, J. E., Casey, B. M. and Sandor, G. G. S. (2007). A population-based study of cardiac malformations and outcomes associated with dextrocardia. *Am. J. Cardiol.* **100**, 305-309.

Boon, M., Smits, A., Cuppens, H., Jaspers, M., Proesmans, M., Dupont, L. J., Vermeulen, F. L., Van Daele, S., Malfroot, A., Godding, V. et al. (2014). Primary ciliary dyskinesia: critical evaluation of clinical symptoms and diagnosis in patients with normal and abnormal ultrastructure. *Orphanet J. Rare Dis.* **9**, 11.

Bouvagnet, P. and de Bellaing, A. M. (2016). Human Genetics of d-Transposition of the Great Arteries. In *Congenital Heart Diseases: The Broken Heart* (ed. S. Rickert-Sperling, R. G. Kelly and D. J. Driscoll), pp. 439-447. Springer Vienna: Vienna.

Brennan, J., Norris, D. P. and Robertson, E. J. (2002). Nodal activity in the node governs left-right asymmetry. *Genes Dev.* **16**, 2339-2344.

Brown, N. A. and Wolpert, L. (1990). The development of handedness in left/right asymmetry. *Development* **109**, 1-9.

Bruneau, B. G., Nemer, G., Schmitt, J. P., Charron, F., Robitaille, L., Caron, S., Conner, D. A., Gessler, M., Nemer, M., Seidman, C. E. et al. (2001). A murine model of holt-oram syndrome defines roles of the t-box transcription factor Tbx5 in cardiogenesis and disease. *Cell* **106**, 709-721.

Cai, C.-L., Liang, X., Shi, Y., Chu, P.-H., Pfaff, S. L., Chen, J. and Evans, S. M. (2003). Isl1 Identifies a cardiac progenitor population that proliferates prior to differentiation and contributes a majority of cells to the heart. *Dev. Cell* **5**, 877-889.

Campione, M., Steinbeisser, H., Schweickert, A., Deissler, K., van Bebber, F., Lowe, L. A., Nowotschin, S., Viebahn, C., Haffter, P., Kuehn, M. R. et al. (1999). The homeobox gene Pitx2: mediator of asymmetric left-right signaling in vertebrate heart and gut looping. *Development* **126**, 1225-1234.

Campione, M., Ros, M. A., Icardo, J. M., Piedra, E., Christoffels, V. M., Schweickert, A., Blum, M., Franco, D. and Moorman, A. F. M. (2001). Pitx2 expression defines a left cardiac lineage of cells: evidence for atrial and ventricular molecular isomerism in the iv/iv mice. *Dev. Biol.* **231**, 252-264.

Chang, H., Zwijsen, A., Vogel, H., Huylebroeck, D. and Matzuk, M. M. (2000). Smad5 is essential for left–right asymmetry in mice. *Dev. Biol.* **219**, 71-78.

Chazaud, C., Chambon, P. and Dollé, P. (1999). Retinoic acid is required in the mouse embryo for left-right asymmetry determination and heart morphogenesis. *Development* **126**, 2589-2596.

Chen, J.-N., van Eeden, F. J. M., Warren, K. S., Chin, A., Nüsslein-Volhard, C., Haffter, P. and Fishman, M. C. (1997). Left-right pattern of cardiac BMP4 may drive asymmetry of the heart in zebrafish. *Development* **124**, 4373-4382.

Chen, C. K., Kühnlein, R. P., Eulenberg, K. G., Vincent, S., Affolter, M. and Schuh, R. (1998). The transcription factors KNIRPS and KNIRPS RELATED control cell migration and branch morphogenesis during Drosophila tracheal. *Development* **125**, 4959-4968.

Chin, A. J., Tsang, M. and Weinberg, E. S. (2000). Heart and gut chiralities are controlled independently from initial heart position in the developing zebrafish. *Dev. Biol.* **227**, 403-421.

Chocron, S., Verhoeven, M. C., Rentzsch, F., Hammerschmidt, M. and Bakkers, J. (2007). Zebrafish Bmp4 regulates left–right asymmetry at two distinct developmental time points. *Dev. Biol.* **305**, 577-588.

Cohen, E. D., Miller, M. F., Wang, Z., Moon, R. T. and Morrisey, E. E. (2012). Wnt5a and Wnt11 are essential for second heart field progenitor development. *Development* **139**, 1931-1940.

Coutelis, J.-B., Morales, N. G., Géminard, C. and Noselli, S. (2014). Diversity and convergence in the mechanisms establishing L/R asymmetry in metazoa. *EMBO Rep.* **15**, 926-937.

Davis, N. M., Kurpios, N. A., Sun, X., Gros, J., Martin, J. F. and Tabin, C. J. (2008). The chirality of gut rotation derives from left-right asymmetric changes in the architecture of the dorsal mesentery. *Dev. Cell* **15**, 134-145.

Deacon, D. C., Nevis, K. R., Cashman, T. J., Zhou, Y., Zhao, L., Washko, D., Guner-Ataman, B., Burns, C. G. and Burns, C. E. (2010). The miR-143-adducin3 pathway is essential for cardiac chamber morphogenesis. *Development* **137**, 1887-1896.

de Boer, B. A., van den Berg, G., de Boer, P. A. J., Moorman, A. F. M. and Ruijter, J. M. (2012). Growth of the developing mouse heart an interactive qualitative and quantitative 3D atlas. *Dev. Biol.* **368**, 203-213.

de Campos-Baptista, M. I. M., Holtzman, N. G., Yelon, D. and Schier, A. F. (2008). Nodal signaling promotes the speed and directional movement of cardiomyocytes in zebrafish. *Dev. Dyn.* **237**, 3624-3633.

de la Cruz, M. V., Sanchez-Gomez, C., Arteaga, M. M. and Argüello, C. (1977). Experimental study of the development of the truncus and the conus in the chick embryo. *J. Anat.* **123**, 661-686.

de la Cruz, M. V., Sanchez-Gomez, C. and Palomino, M. A. (1989). The primitive cardiac regions in the straight tube heart (Stage 9^{-}) and their anatomical expression in the mature heart: an experimental study in the chick embryo. *J. Anat.* **165**, 121-131.

De Luca, A., Sarkozy, A., Consoli, F., Ferese, R., Guida, V., Dentici, M. L., Mingarelli, R., Bellacchio, E., Tuo, G., Limongelli, G. et al. (2010). Familial transposition of the great arteries caused by multiple mutations in laterality genes. *Heart* **96**, 673-677.

de Pater, E., Clijsters, L., Marques, S. R., Lin, Y.-F., Garavito-Aguilar, Z. V., Yelon, D. and Bakkers, J. (2009). Distinct phases of cardiomyocyte differentiation regulate growth of the zebrafish heart. *Development* **136**, 1633-1641.

Digilio, M. C., Casey, B., Toscano, A., Calabrò, R., Pacileo, G., Marasini, M., Banaudi, E., Giannotti, A., Dallapiccola, B. and Marino, B. (2001). Complete transposition of the great arteries: patterns of congenital heart disease in familial precurrence. *Circulation* **104**, 2809-2814.

Domínguez, J. N., Meilhac, S. M., Bland, Y. S., Buckingham, M. E. and Brown, N. A. (2012). Asymmetric fate of the posterior part of the second heart field results in unexpected left/right contributions to both poles of the heart. *Circ. Res.* **111**, 1323-1335.

Felker, A., Prummel, K. D., Merks, A. M., Mickoleit, M., Brombacher, E. C., Huisken, J., Panáková, D. and Mosimann, C. (2018). Continuous addition of progenitors forms the cardiac ventricle in zebrafish. *Nat. Commun.* **9**, 1-14.

Francou, A., Saint-Michel, E., Mesbah, K. and Kelly, R. G. (2014). TBX1 regulates epithelial polarity and dynamic basal filopodia in the second heart field. *Development* **141**, 4320-4331.

Frank, D. U., Fotheringham, L. K., Brewer, J. A., Muglia, L. J., Tristani-Firouzi, M., Capecchi, M. R. and Moon, A. M. (2002). An Fgf8 mouse mutant phenocopies human 22q11 deletion syndrome. *Development* **129**, 4591-4603.

Fujinaga, M. (1997). Development of sidedness of asymmetric body structures in vertebrates. *Int. J. Dev. Biol.* **41**, 153-186.

Fujiwara, T., Dehart, D. B., Sulik, K. K. and Hogan, B. L. M. (2002). Distinct requirements for extra-embryonic and embryonic bone morphogenetic protein 4 in the formation of the node and primitive streak and coordination of left-right asymmetry in the mouse. *Development* **129**, 4685-4696.

Fukui, H., Miyazaki, T., Chow, R. W.-Y., Ishikawa, H., Nakajima, H., Vermot, J. and Mochizuki, N. (2018). Hippo signaling determines the number of venous pole cells that originate from the anterior lateral plate mesoderm in zebrafish. *eLife* **7**, e29106.

Furtado, M. B., Solloway, M. J., Jones, V. J., Costa, M. W., Biben, C., Wolstein, O., Preis, J. I., Sparrow, D. B., Saga, Y., Dunwoodie, S. L. et al. (2008). BMP/SMAD1 signaling sets a threshold for the left/right pathway in lateral plate mesoderm and limits availability of SMAD4. *Genes Dev.* **22**, 3037-3049.

Furtado, M. B., Biben, C., Shiratori, H., Hamada, H. and Harvey, R. P. (2011). Characterization of Pitx2c expression in the mouse heart using a reporter transgene. *Dev. Dyn.* **240**, 195-203.

Galli, D., Dominguez, J. N., Zaffran, S., Munk, A., Brown, N. A. and Buckingham, M. E. (2008). Atrial myocardium derives from the posterior region of the second heart field, which acquires left-right identity as Pitx2c is expressed. *Development* **135**, 1157-1167.

Gibbs, B. C., Damerla, R. R., Vladar, E. K., Chatterjee, B., Wan, Y., Liu, X., Cui, C., Gabriel, G. C., Zahid, M., Yagi, H. et al. (2016). Prickle1 mutation causes planar cell polarity and directional cell migration defects associated with cardiac outflow tract anomalies and other structural birth defects. *Biol. Open* **5**, 323-335.
González-Morales, N., Géminard, C., Lebreton, G., Cerezo, D., Coutelis, J.-B. and Noselli, S. (2015). The atypical cadherin dachsous controls left-right asymmetry in Drosophila. *Dev. Cell* **33**, 675-689.
Grant, M. G., Patterson, V. L., Grimes, D. T. and Burdine, R. D. (2017). Modeling syndromic congenital heart defects in zebrafish. *Curr. Top. Dev. Biol.* **124**, 1-40.
Guerra, A., Germano, R. F., Stone, O., Arnaout, R., Guenther, S., Ahuja, S., Uribe, V., Vanhollebeke, B., Stainier, D. Y. and Reischauer, S. (2018). Distinct myocardial lineages break atrial symmetry during cardiogenesis in zebrafish. *eLife* **7**, 1734.
Guimier, A., Gabriel, G. C., Bajolle, F., Tsang, M., Liu, H., Noll, A., Schwartz, M., El Malti, R., Smith, L. D., Klena, N. T. et al. (2015). MMP21 is mutated in human heterotaxy and is required for normal left-right asymmetry in vertebrates. *Nat. Genet.* **47**, 1260-1263.
Hagen, E. M., Sicko, R. J., Kay, D. M., Rigler, S. L., Dimopoulos, A., Ahmad, S., Doleman, M. H., Fan, R., Romitti, P. A., Browne, M. L. et al. (2016). Copy-number variant analysis of classic heterotaxy highlights the importance of body patterning pathways. *Hum. Genet.* **135**, 1355-1364.
Hami, D., Grimes, A. C., Tsai, H.-J. and Kirby, M. L. (2011). Zebrafish cardiac development requires a conserved secondary heart field. *Development* **138**, 2389-2398.
Harrison, M. J., Shapiro, A. J. and Kennedy, M. P. (2016). Congenital heart disease and primary ciliary dyskinesia. *Paediatr. Respir. Rev.* **18**, 25-32.
Henderson, D. J., Conway, S. J., Greene, N. D. E., Gerrelli, D., Murdoch, J. N., Anderson, R. H. and Copp, A. J. (2001). Cardiovascular defects associated with abnormalities in midline development in the loop-tail mouse mutant. *Circ. Res.* **89**, 6-12.
Hiermeier, F. and Männer, J. (2017). Kinking and torsion can significantly improve the efficiency of valveless pumping in periodically compressed tubular conduits. implications for understanding of the form-function relationship of embryonic heart tubes. *JCDD* **4**, 19-25.
Hildreth, V., Webb, S., Chaudhry, B., Peat, J. D., Phillips, H. M., Brown, N., Anderson, R. H. and Henderson, D. J. (2009). Left cardiac isomerism in the Sonic hedgehog null mouse. *J. Anat.* **214**, 894-904.
Hirokawa, N., Tanaka, Y., Okada, Y. and Takeda, S. (2006). Nodal flow and the generation of left-right asymmetry. *Cell* **125**, 33-45.
His, W. (1868). Die Erste Entwicklung Des Hühnchens Im Ei. Untersuchungen über die erste Anlage des Wirbelthierleibes, Die Erste Entwicklung Des Hühnchens Im Ei, Leipzig, Germany: Vogel.
Hochgreb, T., Linhares, V. L., Menezes, D. C., Sampaio, A. C., Yan, C. Y. I., Cardoso, W. V., Rosenthal, N. and Xavier-Neto, J. (2003). A caudorostral wave of RALDH2 conveys anteroposterior information to the cardiac field. *Development* **130**, 5363-5374.
Hoyle, C., Brown, N. A. and Wolpert, L. (1992). Development of left/right handedness in the chick heart. *Development* **115**, 1071-1078.
Inaki, M., Hatori, R., Nakazawa, N., Okumura, T., Ishibashi, T., Kikuta, J., Ishii, M., Matsuno, K. and Honda, H. (2018). Chiral cell sliding drives left-right asymmetric organ twisting. *eLife Sci.* **7**, e32506.
Isaac, A., Sargent, M. G. and Cooke, J. (1997). Control of vertebrate left-right asymmetry by a snail-related zinc finger gene. *Science* **275**, 1301-1304.
Itasaki, N., Nakamura, H., Sumida, H. and Yasuda, M. (1991). Actin bundles on the right side in the caudal part of the heart tube play a role in dextro-looping in the embryonic chick heart. *Anat. Embryol.* **183**, 29-39.
Ivanovitch, K., Temiño, S. and Torres, M. (2017). Live imaging of heart tube development in mouse reveals alternating phases of cardiac differentiation and morphogenesis. *eLife Sciences* **6**, e30668.
Iwaki, D. D. and Lengyel, J. A. (2002). A Delta-Notch signaling border regulated by Engrailed/Invected repression specifies boundary cells in the Drosophila hindgut. *Mech. Dev.* **114**, 71-84.
Jacobs, J. P., Anderson, R. H., Weinberg, P. M., Walters, H. L., III, Tchervenkov, C. I., Del Duca, D., Franklin, R. C. G., Aiello, V. D., Béland, M. J., Colan, S. D. et al. (2007). The nomenclature, definition and classification of cardiac structures in the setting of heterotaxy. *Cardiol. Young* **17**, 1-28.
Ji, Y., Buel, S. M. and Amack, J. D. (2016). Mutations in zebrafish pitx2 model congenital malformations in Axenfeld-Rieger syndrome but do not disrupt left-right placement of visceral organs. *Dev. Biol.* **416**, 69-81.
Jin, S. C., Homsy, J., Zaidi, S., Lu, Q., Morton, S., DePalma, S. R., Zeng, X., Qi, H., Chang, W., Sierant, M. C. et al. (2017). Contribution of rare inherited and de novo variants in 2,871 congenital heart disease probands. *Nat. Genet.* **49**, 1593-1601.
Juan, T., Géminard, C., Coutelis, J.-B., Cerezo, D., Polès, S., Noselli, S. and Fürthauer, M. (2018). Myosin1D is an evolutionarily conserved regulator of animal left-right asymmetry. *Nat. Commun.* **9**, 1942.
Karner, C. M., Chirumamilla, R., Aoki, S., Igarashi, P., Wallingford, J. B. and Carroll, T. J. (2009). Wnt9b signaling regulates planar cell polarity and kidney tubule morphogenesis. *Nat. Genet.* **41**, 793-799.
Keegan, B. R., Meyer, D. and Yelon, D. (2004). Organization of cardiac chamber progenitors in the zebrafish blastula. *Development* **131**, 3081-3091.
Kelly, R. G., Brown, N. A. and Buckingham, M. E. (2001). The arterial pole of the mouse heart forms from Fgf10-expressing cells in pharyngeal mesoderm. *Dev. Cell* **1**, 435-440.
Kennaway, R., Coen, E., Green, A. and Bangham, A. (2011). Generation of diverse biological forms through combinatorial interactions between tissue polarity and growth. *PLoS Comput. Biol.* **7**, e1002071-e22.
Kennedy, M. P., Omran, H., Leigh, M. W., Dell, S., Morgan, L., Molina, P. L., Robinson, B. V., Minnix, S. L., Olbrich, H., Severin, T. et al. (2007). Congenital heart disease and other heterotaxic defects in a large cohort of patients with primary ciliary dyskinesia. *Circulation* **115**, 2814-2821.
Kidokoro, H., Okabe, M. and Tamura, K. (2008). Time-lapse analysis reveals local asymmetrical changes in C-looping heart tube. *Dev. Dyn.* **237**, 3545-3556.
Kidokoro, H., Yonei-Tamura, S., Tamura, K., Schoenwolf, G. C. and Saijoh, Y. (2018). The heart tube forms and elongates through dynamic cell rearrangement coordinated with foregut extension. *Development* **145**, dev152488-d60.
Kioussi, C., Briata, P., Baek, S. H., Rose, D. W., Hamblet, N. S., Herman, T., Ohgi, K. A., Lin, C., Gleiberman, A., Wang, J. et al. (2002). Identification of a Wnt/Dvl/beta-Catenin –> Pitx2 pathway mediating cell-type-specific proliferation during development. *Cell* **111**, 673-685.
Kitamura, K., Miura, H., Miyagawa-Tomita, S., Yanazawa, M., Katoh-Fukui, Y., Suzuki, R., Ohuchi, H., Suehiro, A., Motegi, Y., Nakahara, Y. et al. (1999). Mouse Pitx2 deficiency leads to anomalies of the ventral body wall, heart, extra- and periocular mesoderm and right pulmonary isomerism. *Development* **126**, 5749-5758.
Koushik, S. V., Wang, J., Rogers, R., Moskophidis, D., Lambert, N. A., Creazzo, T. L. and Conway, S. J. (2001). Targeted inactivation of the sodium-calcium exchanger (Ncx1) results in the lack of a heartbeat and abnormal myofibrillar organization. *FASEB J.* **15**, 1209-1211.
Krebs, L. T., Iwai, N., Nonaka, S., Welsh, I. C., Lan, Y., Jiang, R., Saijoh, Y., O'Brien, T. P., Hamada, H. and Gridley, T. (2003). Notch signaling regulates left-right asymmetry determination by inducing Nodal expression. *Genes Dev.* **17**, 1207-1212.
Latacha, K. S., Rémond, M. C., Ramasubramanian, A., Chen, A. Y., Elson, E. L. and Taber, L. A. (2005). Role of actin polymerization in bending of the early heart tube. *Dev. Dyn.* **233**, 1272-1286.
Lazic, S. and Scott, I. C. (2011). Mef2cb regulates late myocardial cell addition from a second heart field-like population of progenitors in zebrafish. *Dev. Biol.* **354**, 123-133.
Le Garrec, J.-F., Ragni, C. V., Pop, S., Dufour, A., Olivo-Marin, J. C., Buckingham, M. E. and Meilhac, S. M. (2013). Quantitative analysis of polarity in 3D reveals local cell coordination in the embryonic mouse heart. *Development* **140**, 395-404.
Le Garrec, J.-F., Domínguez, J. N., Desgrange, A., Ivanovitch, K. D., Raphaël, E., Bangham, J. A., Torres, M., Coen, E., Mohun, T. J. and Meilhac, S. M. (2017). A predictive model of asymmetric morphogenesis from 3D reconstructions of mouse heart looping dynamics. *eLife Sci.* **6**, e28951-e28935.
Lenhart, K. F., Holtzman, N. G., Williams, J. R. and Burdine, R. D. (2013). Integration of nodal and BMP signals in the heart requires FoxH1 to create left–right differences in cell migration rates that direct cardiac asymmetry. *PLoS Genet.* **9**, e1003109-e11.
Lescroart, F., Kelly, R. G., Le Garrec, J.-F., Nicolas, J.-F., Meilhac, S. M. and Buckingham, M. (2010). Clonal analysis reveals common lineage relationships between head muscles and second heart field derivatives in the mouse embryo. *Development* **137**, 3269-3279.
Lescroart, F., Mohun, T., Meilhac, S. M., Bennett, M. and Buckingham, M. (2012). Lineage tree for the venous pole of the heart: clonal analysis clarifies controversial genealogy based on genetic tracing. *Circ. Res.* **111**, 1313-1322.
Leung, C., Lu, X., Liu, M. and Feng, Q. (2014). Rac1 signaling is critical to cardiomyocyte polarity and embryonic heart development. *J. Am. Heart Assoc.* **3**, e001271-e001271.
Levin, M., Johnson, R. L., Stern, C. D., Kuehn, M. R. and Tabin, C. J. (1995). a molecularpathway determining left-right asymmetry in chick embryogenesis. *Cell* **82**, 803-814.
Levin, M., Pagan, S., Roberts, D. J., Cooke, J., Kuehn, M. R. and Tabin, C. J. (1997). Left/right patterning signals and the independent regulation of different aspects of situs in the chick embryo. *Dev. Biol.* **189**, 57-67.
Li, Y., Klena, N. T., Gabriel, G. C., Liu, X., Kim, A. J., Lemke, K., Chen, Y., Chatterjee, B., Devine, W., Damerla, R. R. et al. (2015). Global genetic analysis in mice unveils central role for cilia in congenital heart disease. *Nature* **521**, 520-524.
Li, D., Sinha, T., Ajima, R., Seo, H.-S., Yamaguchi, T. P. and Wang, J. (2016). Spatial regulation of cell cohesion by Wnt5a during second heart field progenitor deployment. *Dev. Biol.* **412**, 18-31.
Lin, Q., Schwarz, J., Bucana, C. and Olson, E. N. (1997). Control of mouse cardiac morphogenesis and myogenesis by transcription factor MEF2C. *Science* **276**, 1404-1407.

Lin, C. R., Kioussi, C., O'Connell, S., Briata, P., Szeto, D., Liu, F., Izpisúa-Belmonte, J. C. and Rosenfeld, M. G. (1999). Pitx2 regulates lung asymmetry, cardiac positioning and pituitary and tooth morphogenesis. *Nature* **401**, 279-282.
Lin, A. E., Krikov, S., Riehle-Colarusso, T., Frías, J. L., Belmont, J., Anderka, M., Geva, T., Getz, K. D. and Botto, L. D. The National Birth Defects Prevention Study (2014). Laterality defects in the national birth defects prevention study (1998-2007): birth prevalence and descriptive epidemiology. *Am. J. Med. Genet.* **164**, 2581-2591.
Linask, K. K., Yu, X., Chen, Y. and Han, M.-D. (2002). Directionality of heart looping: effects of Pitx2c misexpression on flectin asymmetry and midline structures. *Dev. Biol.* **246**, 407-417.
Linask, K. K., Han, M.-D., Linask, K. L., Schlange, T. and Brand, T. (2003). Effects of antisense misexpression of CFC on downstream flectin protein expression during heart looping. *Dev. Dyn.* **228**, 217-230.
Linask, K. K., Han, M., Cai, D. H., Brauer, P. R. and Maisastry, S. M. (2005). Cardiac morphogenesis: Matrix metalloproteinase coordination of cellular mechanisms underlying heart tube formation and directionality of looping. *Dev. Dyn.* **233**, 739-753.
Logan, M., Pagan-Westphal, S. M., Smith, D. M., Paganessi, L. and Tabin, C. J. (1998). The transcription factor Pitx2 mediates situs-specific morphogenesis in response to left-right asymmetric signals. *Cell* **94**, 307-317.
Long, S., Ahmad, N. and Rebagliati, M. (2003). The zebrafish nodal-related gene southpaw is required for visceral and diencephalic left-right asymmetry. *Development* **130**, 2303-2316.
Lowe, L. A., Yamada, S. and Kuehn, M. R. (2001). Genetic dissection of nodal function in patterning the mouse embryo. *Development* **128**, 1831-1843.
Lu, W., Seeholzer, S. H., Han, M., Arnold, A.-S., Serrano, M., Garita, B., Philp, N. J., Farthing, C., Steele, P., Chen, J. et al. (2008). Cellular nonmuscle myosins NMHC-IIA and NMHC-IIB and vertebrate heart looping. *Dev. Dyn.* **237**, 3577-3590.
Lu, M.-F., Pressman, C., Dyer, R., Johnson, R. L. and Martin, J. F. (1999). Function of Rieger syndrome gene in left-right asymmetry and cranofacial development. *Nature* **401**, 276-278.
Lyons, I., Parsons, L. M., Hartley, L., Li, R., Andrews, J. E., Robb, L. and Harvey, R. P. (1995). Myogenic and morpho.genetic defects in the heart tubes of murlne embryos lacking the homeo box gene. *Genes Dev.* **9**, 1654-1666.
Manasek, F. J., Burnside, B. and Waterman, R. E. (1972). Myocardial cell shape change as a mechanism of embryonic heart looping. *Dev. Biol.* **29**, 349-371.
Männer, J. (2004). On rotation, torsion, lateralization, and handedness of the embryonic heart loop: New insights from a simulation model for the heart loop of chick embryos. *Anat. Rec.* **278A**, 481-492.
Männer, J., Seidl, W. and Steding, G. (1993). Correlation between the embryonic head flexures and cardiac development. An experimental study in chick embryos. *Anat. Embryol.* **188**, 269-285.
Manning, A. and McLachlan, J. C. (1990). Looping of chick embryo hearts in vitro. *J. Anat.* **168**, 257-263.
Martins, P. and Castela, E. (2008). Transposition of the great arteries. *Orphanet J. Rare Dis.* **3**, 27-10.
McCarthy, A. and Brown, N. A. (1998). Specification of left-right asymmetry in mammals: embryo culture studies of stage of determination and relationships with morphogenesis and growth. *Reprod. Toxicol.* **12**, 177-184.
Meilhac, S. M., Kelly, R. G., Rocancourt, D., Eloy-Trinquet, S., Nicolas, J. F. and Buckingham, M. E. (2003). A retrospective clonal analysis of the myocardium reveals two phases of clonal growth in the developing mouse heart. *Development* **130**, 3877-3889.
Meilhac, S. M., Esner, M., Kerszberg, M., Moss, J. E. and Buckingham, M. E. (2004). Oriented clonal cell growth in the developing mouse myocardium underlies cardiac morphogenesis. *J. Cell Biol.* **164**, 97-109.
Meno, C., Shimono, A., Saijoh, Y., Yashiro, K., Mochida, K., Ohishi, S., Noji, S., Kondoh, H. and Hamada, H. (1998). lefty-1 is required for left-right determination as a regulator of lefty-2 and nodal. *Cell* **94**, 287-297.
Meno, C., Takeuchi, J., Sakuma, R., Koshiba-Takeuchi, K., Ohishi, S., Saijoh, Y., Miyazaki, J.-I., ten Dijke, P., Ogura, T. and Hamada, H. (2001). Diffusion of nodal signaling activity in the absence of the feedback inhibitor lefty2. *Dev. Cell* **1**, 127-138.
Merks, A. M., Swinarski, M., Meyer, A. M., Müller, N. V., Özcan, I., Donat, S., Burger, A., Gilbert, S., Mosimann, C., Abdelilah-Seyfried, S. et al. (2018). Planar cell polarity signalling coordinates heart tube remodelling through tissue-scale polarisation of actomyosin activity. *Nat. Commun.* **9**, 1-15.
Mic, F. A., Haselbeck, R. J., Cuenca, A. E. and Duester, G. (2002). Novel retinoic acid generating activities in the neural tube and heart identified by conditional rescue of Raldh2 null mutant mice. *Development* **129**, 2271-2282.
Mine, N., Anderson, R. M. and Klingensmith, J. (2008). BMP antagonism is required in both the node and lateral plate mesoderm for mammalian left-right axis establishment. *Development* **135**, 2425-2434.
Mishra, S. (2015). Cardiac and non-cardiac abnormalities in heterotaxy syndrome. *Indian J. Pediatr.* **82**, 1135-1146.
Mittal, A., Pulina, M., Hou, S.-Y. and Astrof, S. (2013). Fibronectin and integrin alpha 5 play requisite roles in cardiac morphogenesis. *Dev. Biol.* **381**, 73-82.
Mommersteeg, M. T. M., Brown, N. A., Prall, O. W. J., de Gier-de Vries, C., Harvey, R. P., Moorman, A. F. M. and Christoffels, V. M. (2007). Pitx2c and Nkx2-5 are required for the formation and identity of the pulmonary myocardium. *Circ. Res.* **101**, 902-909.
Murray, S. A. and Gridley, T. (2006). Snail family genes are required for left-right asymmetry determination, but not neural crest formation, in mice. *Proc. Natl. Acad. Sci. USA* **103**, 10300-10304.
Nakamura, T. and Hamada, H. (2012). Left-right patterning: conserved and divergent mechanisms. *Development* **139**, 3257-3262.
Nerurkar, N. L., Ramasubramanian, A. and Taber, L. A. (2006). Morphogenetic adaptation of the looping embryonic heart to altered mechanical loads. *Dev. Dyn.* **235**, 1822-1829.
Niederreither, K., Vermot, J., Messaddeq, N., Schuhbaur, B., Chambon, P. and Dollé, P. (2001). Embryonic retinoic acid synthesis is essential for heart morphogenesis in the mouse. *Development* **128**, 1019-1031.
Nishii, K. and Shibata, Y. (2006). Mode and determination of the initial contraction stage in the mouse embryo heart. *Anat. Embryol.* **211**, 95-100.
Noël, E. S., Verhoeven, M., Lagendijk, A. K., Tessadori, F., Smith, K., Choorapoikayil, S., den Hertog, J. and Bakkers, J. (2013). A Nodal-independent and tissue-intrinsic mechanism controls heart-looping chirality. *Nat. Commun.* **4**, 1-9.
Nonaka, S., Tanaka, Y., Okada, Y., Takeda, S., Harada, A., Kanai, Y., Kido, M. and Hirokawa, N. (1998). Randomization of left-right asymmetry due to loss of nodal cilia generating leftward flow of extraembryonic fluid in mice lacking KIF3B motor protein. *Cell* **95**, 829-837.
Norris, D. P., Brennan, J., Bikoff, E. K. and Robertson, E. J. (2002). The Foxh1-dependent autoregulatory enhancer controls the level of Nodal signals in the mouse embryo. *Development* **129**, 3455-3468.
Nowotschin, S., Liao, J., Gage, P. J., Epstein, J. A., Campione, M. and Morrow, B. E. (2006). Tbx1 affects asymmetric cardiac morphogenesis by regulating Pitx2 in the secondary heart field. *Development* **133**, 1565-1573.
Ocaña, O. H., Coskun, H., Minguillón, C., Murawala, P., Tanaka, E. M., Galcerán, J., Muñoz-Chápuli, R. and Nieto, M. A. (2017). A right-handed signalling pathway drives heart looping in vertebrates. *Nature* **549**, 86-90.
Paffett-Lugassy, N., Singh, R., Nevis, K. R., Guner-Ataman, B., O'Loughlin, E., Jahangiri, L., Harvey, R. P., Burns, C. G. and Burns, C. E. (2013). Heart field origin of great vessel precursors relies on nkx2.5 -mediated vasculogenesis. *Nat. Cell Biol.* **15**, 1-10.
Patel, K., Isaac, A. and Cooke, J. (1999). Nodal signalling and the roles of the transcription factors SnR and Pitx2 in vertebrate left–right asymmetry. *Curr. Biol.* **9**, 609-612.
Patten, B. M. (1922). The formation of the cardiac loop in the chick. *Am. J. Anat.* **30**, 373-397.
Phillips, H. M., Rhee, H. J., Murdoch, J. N., Hildreth, V., Peat, J. D., Anderson, R. H., Copp, A. J., Chaudhry, B. and Henderson, D. J. (2007). Disruption of planar cell polarity signaling results in congenital heart defects and cardiomyopathy attributable to early cardiomyocyte disorganization. *Circ. Res.* **101**, 137-145.
Prall, O. W. J., Menon, M. K., Solloway, M. J., Watanabe, Y., Zaffran, S., Bajolle, F., Biben, C., McBride, J. J., Robertson, B. R., Chaulet, H. et al. (2007). An Nkx2-5/Bmp2/Smad1 negative feedback loop controls heart progenitor specification and proliferation. *Cell* **128**, 947-959.
Przemeck, G. K. H. Heinzmann, U., Beckers, J. and Hrabé de Angelis, M. (2003). Node and midline defects are associated with left-right development in Delta1 mutant embryos. *Development* **130**, 3-13.
Pulina, M. V., Hou, S.-Y., Mittal, A., Julich, D., Whittaker, C. A., Holley, S. A., Hynes, R. O. and Astrof, S. (2011). Essential roles of fibronectin in the development of the left–right embryonic body plan. *Dev. Biol.* **354**, 208-220.
Ramasubramanian, A., Chu-Lagraff, Q. B., Buma, T., Chico, K. T., Carnes, M. E., Burnett, K. R., Bradner, S. A. and Gordon, S. S. (2013). On the role of intrinsic and extrinsic forces in early cardiac S-looping. *Dev. Dyn.* **242**, 801-816.
Ramsbottom, S. A., Sharma, V., Rhee, H. J., Eley, L., Phillips, H. M., Rigby, H. F., Dean, C., Chaudhry, B. and Henderson, D. J. (2014). Vangl2-regulated polarisation of second heart field-derived cells is required for outflow tract lengthening during cardiac development. *PLoS Genet.* **10**, e1004871-e16.
Rana, M. S., Théveniau-Ruissy, M., De Bono, C., Mesbah, K., Francou, A., Rammah, M., Domínguez, J. N., Roux, M., Laforest, B., Anderson, R. H. et al. (2014). Tbx1 coordinates addition of posterior second heart field progenitor cells to the arterial and venous poles of the heart. *Circ. Res.* **115**, 790-799.
Rémond, M. C., Fee, J. A., Elson, E. L. and Taber, L. A. (2006). Myosin-based contraction is not necessary for cardiac c-looping in the chick embryo. *Anat. Embryol.* **211**, 443-454.
Ribeiro, I., Kawakami, Y., Büscher, D., Raya, Á., Rodríguez-León, J., Morita, M., Rodríguez Esteban, C. and Izpisúa Belmonte, J. C. (2007). Tbx2 and Tbx3 regulate the dynamics of cell proliferation during heart remodeling. *PLoS ONE* **2**, e398-e310.
Roebroek, A. J., Umans, L., Pauli, I. G., Robertson, E. J., van Leuven, F., Van de Ven, W. J. and Constam, D. B. (1998). Failure of ventral closure and axial rotation in embryos lacking the proprotein convertase Furin. *Development* **125**, 4863-4876.

Rohr, S., Otten, C. and Abdelilah-Seyfried, S. (2008). Asymmetric involution of the myocardial field drives heart tube formation in Zebrafish. *Circ. Res.* **102**, e12-e19.
Ryckebusch, L., Wang, Z., Bertrand, N., Lin, S.-C., Chi, X., Schwartz, R., Zaffran, S. and Niederreither, K. (2008). Retinoic acid deficiency alters second heart field formation. *Proc. Nat. Acad. Sci. USA* **105**, 2913-2918.
Satir, P. (2016). Chirality of the cytoskeleton in the origins of cellular asymmetry. *Philos. Trans. R. Soc. Lond., B, Biol. Sci.* **371**, 20150408-7.
Schoenebeck, J. J., Keegan, B. R. and Yelon, D. (2007). Vessel and blood specification override cardiac potential in anterior mesoderm. *Dev. Cell* **13**, 254-267.
Sefton, M., Sánchez, S. and Nieto, M. A. (1998). Conserved and divergent roles for members of the Snail family of transcription factors in the chick and mouse embryo. *Development* **125**, 3111-3121.
Simmons, O., Snider, P., Wang, J., Schwartz, R. J., Chen, Y. and Conway, S. J. (2015). Persistent Noggin arrests cardiomyocyte morphogenesis and results in early in utero lethality. *Dev. Dyn.* **244**, 457-467.
Simões-Costa, M. S., Vasconcelos, M., Sampaio, A. C., Cravo, R. M., Linhares, V. L., Hochgreb, T., Yan, C. Y. I., Davidson, B. and Xavier-Neto, J. (2005). The evolutionary origin of cardiac chambers. *Dev. Biol.* **277**, 1-15.
Sinha, T., Wang, B., Evans, S., Wynshaw-Boris, A. and Wang, J. (2012). Disheveled mediated planar cell polarity signaling is required in the second heart field lineage for outflow tract morphogenesis. *Dev. Biol.* **370**, 135-144.
Sinha, T., Li, D., Théveniau-Ruissy, M., Hutson, M. R., Kelly, R. G. and Wang, J. (2015). Loss of Wnt5a disrupts second heart field cell deployment and may contribute to OFT malformations in DiGeorge syndrome. *Hum. Mol. Genet.* **24**, 1704-1716.
Sithamparanathan, S., Padley, S. P. G., Rubens, M. B., Gatzoulis, M. A., Ho, S. Y. and Nicol, E. D. (2013). Great vessel and coronary artery anatomy in transposition and other coronary anomalies. *JCMG* **6**, 624-630.
Smith, K. A., Chocron, S., von der Hardt, S., de Pater, E., Soufan, A., Bussmann, J., Schulte-Merker, S., Hammerschmidt, M. and Bakkers, J. (2008). Rotation and asymmetric development of the zebrafish heart requires directed migration of cardiac progenitor cells. *Dev. Cell* **14**, 287-297.
Soh, B.-S., Buac, K., Xu, H., Li, E., Ng, S.-Y., Wu, H., Chmielowiec, J., Jiang, X., Bu, L., Li, R. A. et al. (2014). N-cadherin prevents the premature differentiation of anterior heart field progenitors in the pharyngeal mesodermal microenvironment. *Cell Res.* **24**, 1420-1432.
Soufan, A. T., van den Berg, G., Ruijter, J. M., de Boer, P. A., van den Hoff, M. J. and Moorman, A. F. (2006). Regionalized sequence of myocardial cell growth and proliferation characterizes early chamber formation. *Circ. Res.* **99**, 545-552.
Stainier, D. Y. R., Lee, R. K. and Fishman, M. C. (1993). Cardiovascular development in the zebrafish. *Development* **119**, 31-40.
Stalsberg, H. (1969). The origin of heart asymmetry: right and left contributions of the early chick embryo heart. *Dev. Biol.* **19**, 100-127.
Stennard, F. A., Costa, M. W., Lai, D., Biben, C., Furtado, M. B., Solloway, M. J., McCulley, D. J., Leimena, C., Preis, J. I., Dunwoodie, S. L. et al. (2005). Murine T-box transcription factor Tbx20 acts as a repressor during heart development, and is essential for adult heart integrity, function and adaptation. *Development* **132**, 2451-2462.
Sulik, K., Dehart, D. B., Iangaki, T., Carson, J. L., Vrablic, T., Gesteland, K. and Schoenwolf, G. C. (1994). Morphogenesis of the murine node and notochordal plate. *Dev. Dyn.* **201**, 260-278.
Sun, Y., Liang, X., Najafi, N., Cass, M., Lin, L., Cai, C.-L., Chen, J. and Evans, S. M. (2007). Islet 1 is expressed in distinct cardiovascular lineages, including pacemaker and coronary vascular cells. *Dev. Biol.* **304**, 286-296.
Taniguchi, K., Maeda, R., Ando, T., Okumura, T., Nakazawa, N., Hatori, R., Nakamura, M., Hozumi, S., Fujiwara, H. and Matsuno, K. (2011). Chirality in planar cell shape contributes to left-right asymmetric epithelial morphogenesis. *Science* **333**, 339-341.
Thompson, R. P., Abercrombie, V. and Wong, M. (1987). Morphogenesis of the truncus arteriosus of the chick embryo heart: movements of autoradiographic tattoos during septation. *Anat. Rec.* **218**, 434-440.
Tsukui, T., Capdevila, J., Tamura, K., Ruiz-Lozano, P., Rodriguez-Esteban, C., Yonei-Tamura, S., Magallón, J., Chandraratna, R. A., Chien, K., Blumberg, B. et al. (1999). Multiple left-right asymmetry defects in Shh(−/−) mutant mice unveil a convergence of the shh and retinoic acid pathways in the control of Lefty-1. *Proc. Natl Acad. Sci. USA* **96**, 11376-11381.
Van Praagh, S. (2006). Cardiac malpositions and the heterotaxy syndromes. In *Nadas' Pediatric Cardiology* (ed. J. F. Keane, J. E. Lock and D. C. Fyler), pp. 589-608. Philadelphia: Saunders Elsevier Inc.
van Vliet, P. P., Lin, L., Boogerd, C. J., Martin, J. F., Andelfinger, G., Grossfeld, P. D. and Evans, S. M. (2017). Tissue specific requirements for WNT11 in developing outflow tract and dorsal mesenchymal protrusion. *Dev. Biol.* **429**, 249-259.
von Both, I., Silvestri, C., Erdemir, T., Lickert, H., Walls, J. R., Henkelman, R. M., Rossant, J., Harvey, R. P., Attisano, L. and Wrana, J. L. (2004). Foxh1 is essential for development of the anterior heart field. *Dev. Cell* **7**, 331-345.
Veerkamp, J., Rudolph, F., Cseresnyes, Z., Priller, F., Otten, C., Renz, M., Schaefer, L. and Abdelilah-Seyfried, S. (2013). Unilateral dampening of Bmp activity by nodal generates cardiac left-right asymmetry. *Dev. Cell* **24**, 660-667.
Vincent, S. D., Norris, D. P., Ann Le Good, J., Constam, D. B. and Robertson, E. J. (2004). Asymmetric Nodal expression in the mouse is governed by the combinatorial activities of two distinct regulatory elements. *Mech. Dev.* **121**, 1403-1415.
Voronov, D. A., Alford, P. W., Xu, G. and Taber, L. A. (2004). The role of mechanical forces in dextral rotation during cardiac looping in the chick embryo. *Dev. Biol.* **272**, 339-350.
Waldo, K. L., Kumiski, D. H., Wallis, K. T., Stadt, H. A., Hutson, M. R., Platt, D. H. and Kirby, M. L. (2001). Conotruncal myocardium arises from a secondary heart field. *Development* **128**, 3179-3188.
Waldo, K. L., Hutson, M. R., Stadt, H. A., Zdanowicz, M., Zdanowicz, J. and Kirby, M. L. (2005). Cardiac neural crest is necessary for normal addition of the myocardium to the arterial pole from the secondary heart field. *Dev. Biol.* **281**, 66-77.
Wallis, G. A., Debich-Spicer, D. and Anderson, R. H. (2011). Congenitally corrected transposition. *Orphanet J. Rare Dis.* **6**, 22.
Wang, J., Mark, S., Zhang, X., Qian, D., Yoo, S.-J., Radde-Gallwitz, K., Zhang, Y., Lin, X., Collazo, A., Wynshaw-Boris, A. et al. (2005). Regulation of polarized extension and planar cell polarity in the cochlea by the vertebrate PCP pathway. *Nat. Genet.* **37**, 980-985.
Yamamoto, M., Mine, N., Mochida, K., Sakai, Y., Saijoh, Y., Meno, C. and Hamada, H. (2003). Nodal signaling induces the midline barrier by activating Nodal expression in the lateral plate. *Development* **130**, 1795-1804.
Yan, Y.-T., Gritsman, K., Ding, J., Burdine, R. D., Corrales, J. D., Price, S. M., Talbot, W. S., Schier, A. F. and Shen, M. M. (1999). Conserved requirement for EGF–CFC genes in vertebrate left–right axis formation. *Genes Dev.* **13**, 2527-2537.
Yu, X., St Amand, T. R., Wang, S., Li, G., Zhang, Y., Hu, Y. P., Nguyen, L., Qiu, M. S. and Chen, Y. P. (2001). Differential expression and functional analysis of Pitx2 isoforms in regulation of heart looping in the chick. *Development* **128**, 1005-1013.
Yue, X., Schultheiss, T. M., McKenzie, E. A. and Rosenberg, R. D. (2004). Role of heparan sulfate in dextral heart looping in chick. *Glycobiology* **14**, 745-755.
Zaffran, S., Kelly, R. G., Meilhac, S. M., Buckingham, M. E. and Brown, N. A. (2004). Right ventricular myocardium derives from the anterior heart field. *Circ. Res.* **95**, 261-268.
Zhou, W., Lin, L., Majumdar, A., Li, X., Zhang, X., Liu, W., Etheridge, L., Shi, Y., Martin, J., Van de Ven, W. et al. (2007). Modulation of morphogenesis by noncanonical Wnt signaling requires ATF/CREB family–mediated transcriptional activation of TGFβ2. *Nat. Genet.* **39**, 1225-1234.
Zhou, Y., Cashman, T. J., Nevis, K. R., Obregon, P., Carney, S. A., Liu, Y., Gu, A., Mosimann, C., Sondalle, S., Peterson, R. E. et al. (2011). Latent TGF-β binding protein 3 identifies a second heart field in zebrafish. *Nature* **474**, 645-648.